



MASTER THESIS IN NANOSCIENCE

---

# Two Dimensional Brain-On-Chip Model

Towards Remodelling of the Nigrostriatal Pathway to Study Parkinson's  
Disease

---

*Written by*

Sebastian Buchmann

*Supervised by*

Janko Kajtez

Prof. Dr. Jenny Emnéus

Prof. Dr. Henning Stahlberg

May 4, 2019

## Abstract

Parkinson's disease is a complex neurodegenerative disorder. The development is not fully understood and there is currently no method to cure it. In people suffering from Parkinson's disease the nigrostriatal pathway is damaged. More precisely, dopaminergic neurons from substantia nigra projecting to the striatum are degenerated. The resulting lack of dopamine causes impairments of motor functions.

The degeneration of dopaminergic neurons has mostly been investigated using animal models or cell-based *in vitro* models. To better understand the nigrostriatal pathway a more complex physiological *in vitro* environment is needed. Existing neurite guidance microfluidic chip technologies allow the study of neurite growth. However, chips fabricated with conventional methods do not allow to directly access the cells and are composed of a high amount of polydimethylsiloxane (PDMS). Not fully crosslinked PDMS can be toxic to cells.

We developed a novel microfluidic chip fabrication method by combining PDMS 3D printing with replica moulding. The method allowed precise deposition of small amounts of PDMS onto a micro patterned master mould. Thereafter, we were able to fabricate a neurite guidance chip with minimized amount of PDMS and open wells. Cells that only lived for 3 days on a PDMS based chip obtained by conventional replica moulding were still alive after 40 days on the new chip.

We differentiated human neural stem cells in two compartments that were connected by neurite guidance grooves into cells having characteristics of the forebrain and the midbrain region, respectively. Dopaminergic neurons grew from the compartment representing the midbrain region through the grooves into the compartment of the forebrain cells, where many cells differentiated into astrocytes.

The presented model mimicking parts of the nigrostriatal pathway could be used for further studies helping to understand the degeneration of dopaminergic neurons as well as the influence of astrocytes in Parkinson's disease. The newly developed method for microfluidic chip production opens up new possibilities for fabricating more complex PDMS based microfluidic structures.

## **Acknowledgement**

I would like to thank Janko Kajtez for the direct supervision during my master's project, introducing me into the field of stem cell culture and neurite guidance chip fabrication, performing the PDMS printing, supporting me throughout the whole work progress and patiently answering all my questions.

I would like to thank Prof. Dr. Jenny Ennéus for the possibility to join and work in the Bioanalytics group at DTU and the supervision of my Master's Thesis together with Prof. Dr. Henning Stahlerg and Dr. Thomas Braun as supervisors from the University of Basel.

I would further like to thank all the group and lab members for the welcoming and warm work environment. Especially, Shashank Vasudevan for fabricating the master moulds in the clean room, Naricha Pupinyo for introducing me into micro milling and Arto Heiskanen for sharing his experience and expertise throughout the whole project.

I would also like to thank my father for reading through the thesis and spell checking my writing.

# Contents

<b>1</b>	<b>Introduction</b>	<b>1</b>
1.1	Modelling Parkinson’s Disease . . . . .	3
1.2	Compartmentalized Neurite Guidance Chip . . . . .	4
1.3	Microfluidic Chip Fabrication . . . . .	6
<b>2</b>	<b>Novel Method for Neurite Guidance Chip Fabrication</b>	<b>8</b>
2.1	Open Well Design . . . . .	9
2.2	3D Printed Soft Lithography . . . . .	10
2.3	Different Well-Extension Materials . . . . .	12
2.4	Hot Embossed PMMA Chip . . . . .	14
2.5	Discussion and Conclusion . . . . .	16
<b>3</b>	<b>HNS1 Cell Viability Analysis</b>	<b>17</b>
3.1	PDMS Toxicity . . . . .	17
3.2	Long-Term Differentiation of hNS1 Cells . . . . .	20
3.3	Discussion and Conclusion . . . . .	21
<b>4</b>	<b>Characterization of the two Cell Population</b>	<b>22</b>
<b>5</b>	<b>Reconstructing the Nigrostriatal Pathway</b>	<b>26</b>
5.1	Seeding Optimization . . . . .	26
5.2	Microgroove for Directional Growth . . . . .	26
5.3	Nigrostriatal Pathway . . . . .	29
<b>6</b>	<b>Conclusion and Outlook</b>	<b>31</b>
<b>7</b>	<b>Materials and Methods</b>	<b>33</b>
7.1	Soft Lithography . . . . .	33
7.1.1	Master Mould Fabrication . . . . .	33
7.1.2	Conventional Replica Moulding . . . . .	33
7.1.3	3D Printed Replica Moulding . . . . .	33
7.2	PLA Printing . . . . .	34
7.3	Micromilling . . . . .	34
7.4	Hot Embossing . . . . .	34
7.5	Chip Assembly . . . . .	34
7.6	PDMS Washing Procedure . . . . .	35
7.7	Cell Culture . . . . .	35
7.8	Immunocytochemistry . . . . .	37
7.9	Optical and Fluorescent Imaging and Image Analysis . . . . .	38
<b>8</b>	<b>References</b>	<b>39</b>

# 1 Introduction

It was in 1817 when James Parkinson published a clinical description of 6 patients with the title “An Essay on the Shaking Palsy” [1]. He described in detail the involuntary motions of patients suffering from the malady, which today is known as the Parkinson’s disease (PD) [2]. After Alzheimer disease, PD is the second most common neurodegenerative disorder [3]. Approximately 0.3% of the population in industrialized countries suffer from PD and with higher age the percentage of people is increased drastically to 1% of people over 60 years and to 10% of people over 80 [4]. With ageing population, the impact of PD will continuously increase and with it the socioeconomic costs [5].

PD is usually diagnosed by impaired motor functions, which include slowed down movements (bradykinesia), rigidity, tremor and instability. Recently, nonmotor symptoms such as depression, cognitive decline and sleep disturbance have also been recognized as symptoms of PD [6]. However, a definitive diagnose at early stages does not exist [4, 6]. The gold standard for diagnosis is post-mortem pathological examination [6, 7]. The hallmark of PD is the loss of dopaminergic neurons in substantia nigra pars compacta (SNc). SNc is a subregion located in the midbrain and important for motor functions. Usually 50-70% of the neurons from substantia nigra have been lost by the time of death in comparison to an unaffected brain [7]. The dopaminergic neurons projecting to the striatum are also known as the nigrostriatal pathway (see figure 1). It is the degeneration of the nigrostriatal pathway and the resulting loss of dopamine in the striatum causing impairment in motor functions [4].

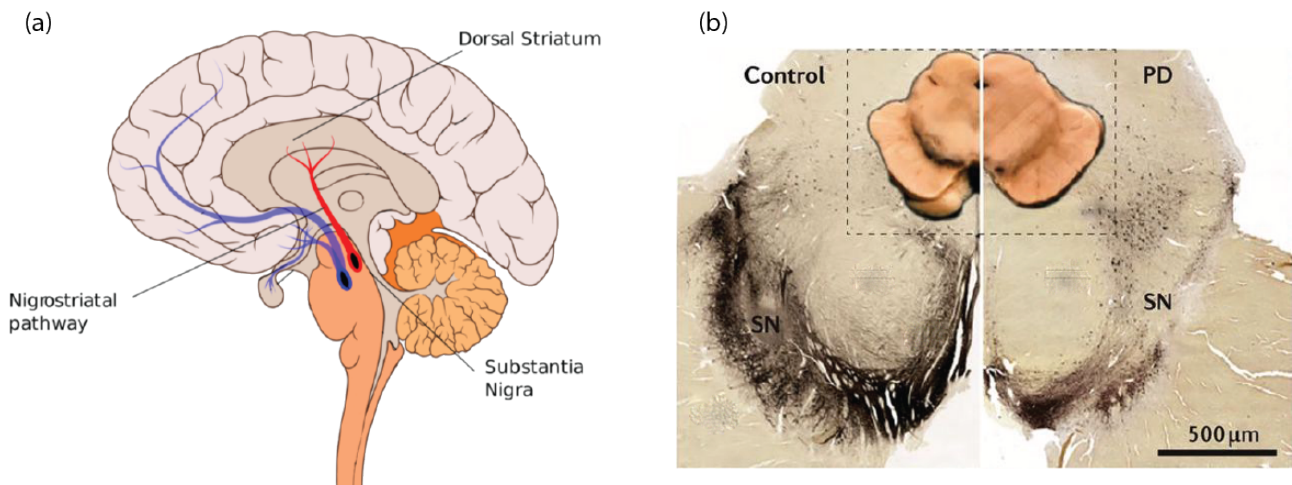


Figure 1: (a) Schematic cross section illustration of a brain showing the nigrostriatal pathway (adapted from [8]). (b) Transverse section of the midbrain comparing a PD brain with a healthy brain and showing the loss of dopaminergic neurons (adapted from [9]).

A second pathological hallmark is the presence of Lewy bodies. Lewy bodies are misfolded aggregates mostly consisting of  $\alpha$ -synuclein. The exact role of Lewy bodies is still unknown [4, 6]. It has often been proposed that Lewy bodies can cause the neuronal degeneration. However, newer studies led to the conclusion that the pathology is more complex. There are alternative forms of  $\alpha$ -synuclein aggregation and thus only certain forms could be toxic for neurons [4]. Studies analysing 3D molecular structures of mutated  $\alpha$ -synuclein even question whether they are able to aggregate [10]. Other features such as oxidative stress, neuroinflammation, excitotoxicity and altered mitochondrial functions have been shown to have an influence in the loss of SNc neurons [4]. Additionally, monogenetic forms of PD

caused by *parkin* or *LRRK2* mutations have been identified where no Lewy bodies were found at all [6]. The different factors that could lead to PD will not be further discussed in more details but are mentioned here to underline the complexity of PD and the lack of knowledge about the origin and development of the disease. Further research in understanding the mechanism in more detail is thus necessary and inevitable for a continually ageing population.

It is well known that currently there is no method to cure PD. Current treatments are only able to increase the quality of life of PD patients through the treatment of the symptoms. There are several dopaminergic agents available that can enhance dopamine concentration or stimulate dopamine receptors to decrease the motor symptoms [6, 11]. The most effective treatment for many years has been the combination of levodopa and a peripheral decarboxylase inhibitor [7]. However, long term therapies can also cause severe motor complications as side-effects as well as impulse control disorders such as gambling, hypersexuality or binge eating. In late stages of the disease, levodopa-resistant symptoms can be detected [6]. Besides the drug-based treatments, surgical treatment strategies do exist, which are mostly used in later stages. High-frequency deep brain stimulations (DBS) of specific areas of the brain can be performed by inserting an electrode. DBS has the great benefit of being adjustable and reversible [12]. The operation however is technically difficult and there are concerns about the increased incidents of psychiatric side effects [7].

Besides focusing on treating symptoms, lots of effort has been invested in finding solutions to repair degenerated neurons. Attempts were carried out by delivering glial-cell-derived neurotrophic factors (GDNF) to hinder the degeneration as well as promote re-growth of dopaminergic cells. However, clinical trials where GDNF has been infused into patient's brain did not show any significant changes over a period of 6 months [12]. A major research interest in the last years has been curing PD using cell therapies. Fetal ventral mesencephalic (VM) tissue and stem cells can serve for transplantation and replacement of dopaminergic innervation of the striatum [13, 14]. It has been reported that two patients who received foetal VM tissue transplants showed improvements in PD symptoms in the fourth year after the operation and had no need for dopaminergic medications after 16 and 5 years respectively [15]. Despite the fact that both patients suffered from graft-induced dyskinesia, poor availability of embryonic fetuses and most importantly ethical issues, using foetal VM tissue does not serve as a long-term mass solution. The use of stem cells has been considered as a promising alternative option. They can self-renew and differentiate into various types of cells. The aim is to develop stem cell-based culture protocols that result in functional and transplantable cells. However, potential hazards such as immune rejection and tumour formation do exist. Embryonic stem cells, neural precursor cells as well as induced pluripotent stem cells could be used [14].

To summarize, it is neither fully understood why and how the highly complex PD occurs nor is there a cure for it. The current symptom treatment strategies have many negative side effects in the long term. The already big impact of PD on today's society will continuously increase with ageing population. This underlines the importance to continue research in understanding better the development as well as possible treatment therapies of PD. Out of many different approaches we would like to highlight the importance of developing reliable PD models, which can be used to discover new insights regarding understanding as well as treating PD. Different approaches in modelling PD will be discussed in the following paragraph, which in the end will lead to the description of our approach in developing a method to remodel PD.

## 1.1 Modelling Parkinson's Disease

For a better understanding of PD in regard to the pathogenesis as well as potential therapies, models of PD are very important. In fact, many new discoveries about PD have already been made thanks to a large amount of studies based on different PD models. The degeneration of the nigrostriatal pathway is one of major components of PD. Concerning animal based models, neurotoxins affecting the dopaminergic neurons have been and still are being used to disrupt the nigrostriatal pathway.

Reserpine was found to cause a temporary akinetic state in rabbits. With the help of it, it was shown that L-DOPA eased the induced akinetic state and it was thus hypothesised that it is the dopamine depletion causing the motor symptoms [16, 17]. Irreversible neurotoxins such as 6-hydroxydopamine (6-OHDA), 1-methyl-4-phenyl-1,2,3,6-tetrahydropyridine (MPTP) or rotenone are also widely used to destroy the nigrostriatal pathway [18, 19]. 6-OHDA was the first chemical agent that was discovered to have neurotoxic effects on the nigrostriatal pathway. By injection into the striatum, progressive damage in the nigrostriatal pathway is visible over a time of 3 weeks. Additionally, nonmotor symptoms of PD have also been recorded. It is important to mention that Lewy bodies are not formed in this model [18, 16]. The neurotoxic effect of MPTP was discovered in the 1980s when drug users in California showed symptoms of PD after intravenous injection of drugs that were contaminated with MPTP [18, 20]. Postmortem examinations of the mentioned cases showed the loss of the nigrostriatal pathway as in people who suffered from PD. Until today MPTP is used for preclinical tests for new therapeutic strategies in various mammalian species, where it damages the nigrostriatal dopaminergic pathway and produces PD-like effects [18].

In neurotoxin based PD models the age-dependent progression as well as Lewy body formation are typically not seen. After the discovery of monogenic form of PD, transgenic animals have been served as new animal models [20]. *Drosophila* that were over expressing  $\alpha$ -synuclein or that were induced with the  $\alpha$ -synuclein mutation linked to PD showed  $\alpha$ -synuclein accumulations which resembled Lewy bodies as well as age-dependent loss of dopaminergic neurons [21, 22]. Many genetic mouse models have also been developed since then. A few examples are mutations in the gene for leucine-rich repeat serine/threonine kinase 2 (LRRK2) that cause autosomal dominant PD. Up to 100 disease-causing mutations are known in the Parkin gene causing autosomal recessive form of PD. Additionally, multiple transgenic mouse lines have been developed [20]. Even though genetic mutations in PD are only present in roughly 10% of the cases, studying those mutations could help us understand the complex development of PD [19]. Animal-based models of PD have been crucial and irreplaceable in the study of the disease but they have inherent limitations. Performing live *in vivo* observations on a molecular level is limited to a certain amount of imaging techniques. Trying to understand PD in more detail the animals models already seem to be too complex. The degree and size of the induced injury, which is difficult to precisely replicate in animal models, has a big influence on the healing process and can make these models inconsistent [23, 24]. Ethical considerations and thus high regulatory barriers as well as high animal housing costs should also be considered [24]. *In vitro* models can here be used as a very helpful alternative. Many studies on a cellular level evaluating the influence of neurotrophic factors, oxidative stress and  $\alpha$ -synuclein aggregation are being performed with primary cells and stem cells and provide new important insights [25, 26, 27]. Compared to animal models they do lack a certain complexity regarding cellular arrangements when using multiple cell lines and are mostly performed in conventional well culture plates.

Combining cellular models with lab-on-a-chip devices allow to insert a certain complexity level. Neural cell growth combined with microfluidic devices allow to observe and examine the development and growth of neurons under different conditions [28, 29]. Different neurite guidance *in vitro* approaches and how they could be used as a PD models will be discussed in the following paragraph.

## 1.2 Compartmentalized Neurite Guidance Chip

Lab-on-chip devices such as neurite guidance chips provide a platform to mimic and investigate organic systems. A milestone in microfluidic platforms for neuronal culture was performed in 2005/2006 by Anne M. Taylor and Jeong Won Park [28, 29]. They designed a simple two-compartment chip where the two compartments (axonal and somal side) were connected with micrometre-sized grooves. Axons were able to grow through the grooves into the other compartment (see figure 2 a). One compartment could be fluidically isolated from the other by inducing small hydrostatic pressure differences. The chip was fabricated using the concept of polydimethylsiloxane (PDMS) based soft-lithography and is nowadays commercially available. The relatively simple chip could be fabricated within a few days, allowing rapid prototyping. Therefore, many other research groups used this basic concept for further studies. In this part of this thesis, different studies will be described where the basic chip design has been used and where some novel applications have been added.

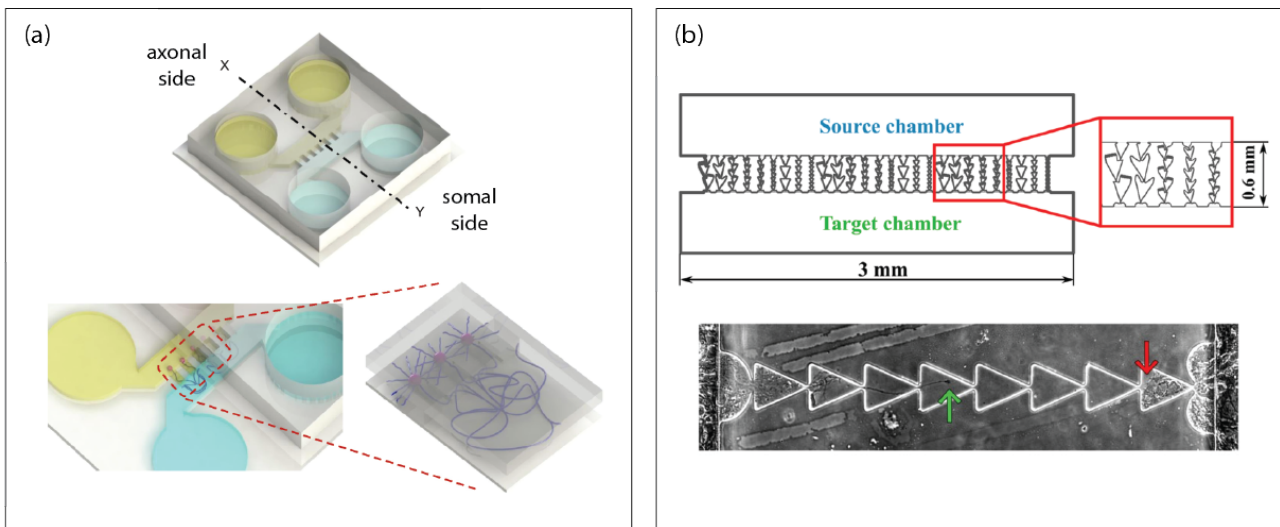


Figure 2: (a) Model illustrating the design of the first PDMS based compartmentalized neurite guidance chip. The two compartments have open round wells to access the cell media and are connected through small grooves in the middle channel part (adapted from [30]). (b) Figure showing differently shaped grooves to promote one-directional neurite growth (adapted from [31]).

Kim *et al.* used the compartmentalized culture platform to examine the regeneration of injured central nervous system neurons. Rat cortical neurons were cultured in one compartment (somal side) for 7 days. Axons grew through the grooves into the second compartment (axonal side) where they were cut off by vacuum aspiration of the media in the axonal side. They were then able to monitor the regeneration of injured axons under different conditions [32]. Southam *et al.* used the same chip design to model neuromuscular signalling processes using primary rat cells. They managed to culture motor neurons in one compartment. From there axons grew into the second compartment where they

connected to skeletal muscle cells [33]. Another research group managed to investigate the neuron-to-neuron transport of miss-folded  $\alpha$ -synuclein that is involved in PD [34].

Adaptations to the basic design for different studies have also been performed. By introducing asymmetrical shapes into the grooves connecting the two compartments one research group managed to influence the directional growth of axons from one compartment into the other [31] (see figure 2 b). The conventional design has closed channels. Therefore, it is not possible to directly physically access the cells next to the guiding grooves. To do so Yang *et al.* introduced a simple open well design consisting of two open squared wells which were connected by the microgrooves. The open wells were manually cut out of the PDMS chip obtained by soft-lithography. The direct access to the cells allowed them to introduce an electrode for electrical stimulation, which increased myelin segment formation [35].

In our work we wanted to use the compartmentalized microfluidic chip design to mimic the nigrostriatal pathway which could be used as a potential PD model. Similarly, as performed in the above mentioned examples we wanted to coculture two different cell lines and induce directional neurite growth from one compartment (containing cells representing SNc) to the second compartment (containing cells representing striatum). In contrast to the earlier described models where primary animal cells were used, we wanted to use two human neural stem cell strains that differentiate on the chip into corresponding dopaminergic cells of the substantia nigra and non-dopaminergic cells of the striatum, respectively. Using neural progenitors had the advantage of relatively simpler and shorter differentiation into neurons compared to pluripotent stem cells. The stem cells (hVM1 and hNS1) were derived from the VM and the forebrain of a 10 and 10.5 weeks old foetus, respectively [36, 37, 38]. However, earlier work in this lab showed that it was not possible to cultivate and differentiate hNS1 cells on a standard PDMS-based compartmentalized neurite guidance chip. Even on the commercially available PDMS chip from Xona microfluidics the cells died within a few days after seeding. Excessive washing and/or pre-soaking in cell culture media did not increase the cell viability either. Changing the cell line would have been a possible option but at the same time it meant that hNS1 cells were good indicators to measure PDMS toxicity. Even if PMDS does not induce cell death to other cell lines, it could be very likely that it interferes with gene expression and cellular processes. This could alter the experiment without our knowledge. For that reason we considered different materials and fabrication approaches to obtain a neurite guidance chip, where PDMS does not negatively affect the cells. Different method and materials exist that could be used to fabricate microfluidic chips. In the last part of the introduction an overview about different approaches will be given and their advantages and disadvantages will be discussed.

### 1.3 Microfluidic Chip Fabrication

Microfluidic chip designs serve as miniaturized systems for biological as well as chemical analysis. Due to the small size, portable devices and parallel operations for higher throughput are easily achieved. Additionally, small sample and reagent volumes are needed resulting in a low waste level [39]. Important features that should be considered when deciding on the material as well as the fabrication methods are the minimal structural resolution, material costs, production time, sufficient transparency for imaging purposes, flexibility in changing and modifying the design and most importantly, for biological applications, the material has to be biocompatible [40].

Soft lithography in combination with PDMS replica moulding is one of the most popular and widely used approaches for microfluidic chip fabrications. A silicon master is patterned using photolithography. Usually a silicon wafer is coated with a photoresist such as SU-8. By exposing SU-8 to ultraviolet light (UV) through a mask one can obtain structures down to one micrometre. Applying multiple steps of photoresist coating and UV exposure makes it possible to obtain structures with height differences from a few micrometres up to several hundred micrometres. A two-component mixture of PMDS and cross-linking agent is poured on the Si-master mould. After hardening the imprinted PDMS can be peeled off (see figure 3). PDMS can be cut and punched easily into the desired shape and then bonded on a glass substrate to enclose the channels. Bonding on glass can be performed reversibly or covalently by using plasma activation [39]. The optical transparency as well as the low elastic modulus of PDMS makes it very convenient for imaging as well inserting valves and tubing systems [41, 42].

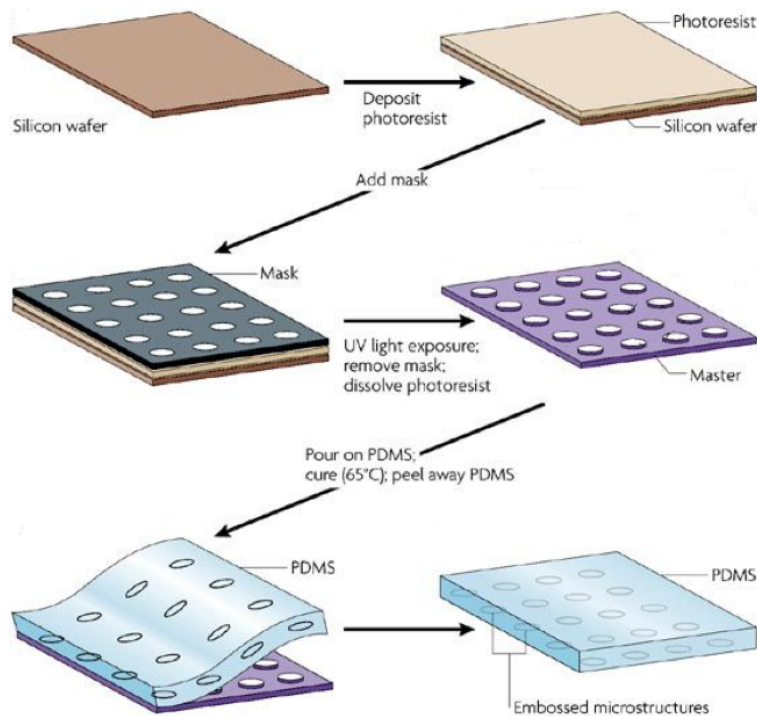


Figure 3: Illustration showing the concept of softlithography. PDMS is moulded onto a master mould obtained by photolithography. After being fully cured, microstructured PDMS can be peeled off (adapted from [43]).

For applications with cells, however, PDMS has some very important drawbacks. PDMS does adsorb hydrophobic molecules such as lipids, essential amino acids, vitamins, hormones and growth factors. The adsorption of such molecules can disturb the cell culture conditions [44, 45]. Additionally, it has been measured that small non-crosslinked PDMS oligomers leach out of bulk PDMS into the culture media and can be taken up by cells into the membrane within 24 hours [46]. By applying several long term solvent extraction methods to reduce the amount of non-crosslinked oligomers, a small amount of oligomers still remains in PDMS, which later can be detected in cell culture media [46, 47]. Millet *et al.* managed to increase the cell viability of primary neurons in a PDMS chip from less than two up to eleven days [48]. However, for long term stem cell differentiation processes this is not a sufficient time. Besides the fact that the washing processes for PDMS are long and tedious and introduce the danger of remaining solvents killing the cells, they do not fully remove the non-crosslinked oligomers. Therefore, if a cell line (such as hNS1) is very sensitive to non-crosslinked oligomers, the amount of PDMS should be minimized or if possible, it should be completely avoided. It is worth notifying that the company xona microfluidics who offered the first commercially available neurite guidance chips made out of PDMS just recently, in 2018, launched a new injection moulded plastic chip which is claimed to be specially suited for sensitive human stem cell-derived neurons [49]. Since we wanted to make modification regarding the grooves for one-directional guidance and their chip only contained straight grooves, it did not serve any purpose for our approach. Additionally, since the channels next to the grooves are closed it would have not been possible to directly access them.

Thermoplastic polymers such as polymethyl methacrylate (PMMA), polycarbonate, polystyrene, or cyclic olefin copolymer could serve as an alternative option. Thermoplastic chips could be prepared by using fabrication techniques such as injection moulding, hot embossing or micro milling [50]. Using injection moulding, high resolution and high aspect ratios can be obtained. For large scale production, injection moulding is a very cost effective option. Once a mould is fabricated, it is very easy to produce many chips. However, in a prototype phase where one wants to be flexible in quickly changing the design, this would be a very expensive method [51]. Therefore, injection moulding did not seem to be a reasonable choice as an alternative fabrication method. Micromilling has a resolution limitation in the lower micrometre scale [52]. Therefore, it would not be possible to make slight changes of the groove design, for example adding directional asymmetrical shapes instead of only having straight microgrooves. For the concept of hot embossing, just as for soft lithography, a SU-8 patterned Si-master could also be used to imprint structures in sufficiently enough resolution. For thermoplastics the bonding strategy is more difficult in comparison to PDMS. They do not form conformal contact with other surfaces. Thermal bonding as well as chemical bonding (chemical welding) can be performed, however finding optimal parameters for small structures can be challenging [50, 53].

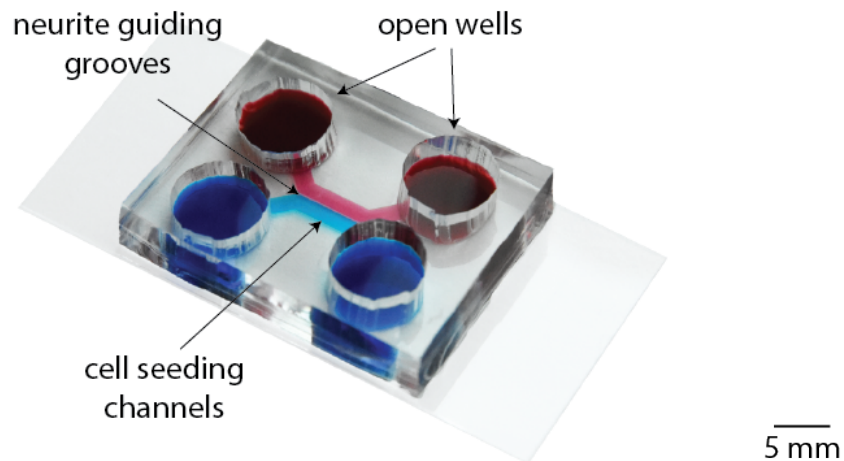
A newer method to fabricate microfluidic chips is using 3D printing techniques such as filament printer or stereolithography. However, until today 3D printing techniques have an x-y resolution of a few tenths of micrometres, which is also not sufficient for our purpose [54, 55].

In this work we aimed to remodel the nigrostriatal pathway using a neurite guidance chip. The PDMS toxicity pushed us in developing a new approach for microfluidic chip fabrication. The novel method allowed us to minimize toxic PDMS content and we were therefore able to differentiate sensitive human neural stem cells on the chip. The fabrication work progress of the neurite guidance chip and analysis of the nigrostriatal pathway model will be presented here.

## 2 Novel Method for Neurite Guidance Chip Fabrication

To remodel the nigrostriatal pathway we wanted to differentiate two human stem cell lines (hNS1 and hVM1) on a neurite guidance chip into neurons having characteristics of SNc, which connect through neurite extensions with neurons having characteristics of the striatum. The biggest challenge we faced in our approach of remodelling the nigrostriatal pathway was the viability of the cell line representing the striatum (hNS1 cells). The cells differentiated well in conventional well plates. However, on the neurite guidance chips obtained by PDMS soft lithography (more precise replica moulding) the cells died within a few days (see figure 4). Cell death usually started from one or two spots and then spread out quickly to the other cells. Based on information found in the literature (as described in the introduction section 1.3) we assumed that PDMS has a toxic effect on the hNS1 cells. Other possible negative effects could have been due to a low nutrition availability in the closed channels containing only a small amount of media volume or that too high flow disturbance occurs in the cell seeding channels when the media is changed .

(a)



(b) hNS1 cells on chip

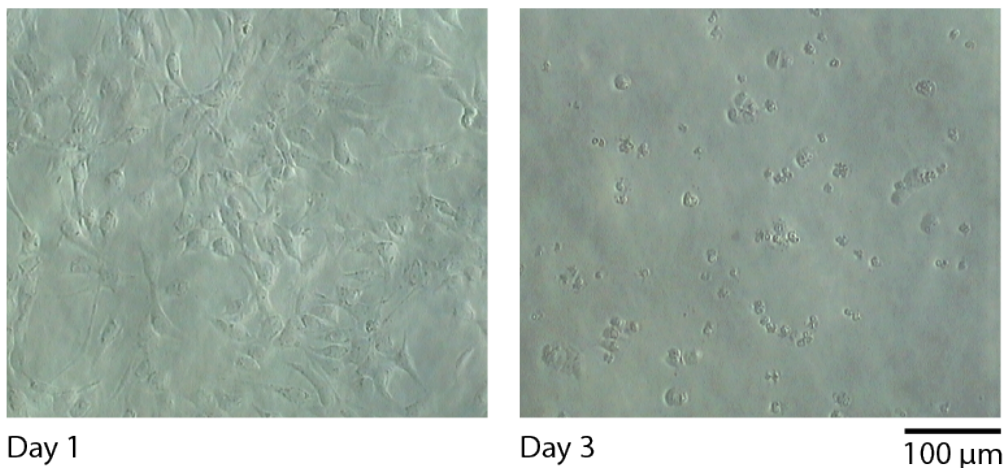


Figure 4: (a) Neurite guidance microfluidic chip with open round well to seed the cells into the two closed channels, which are connected through neurite guiding grooves. (b) HNS1 cells seeded in the channel of the chip after one day and three days, where they had already died.

For that reason, we started a series of different approaches to increase the cell viability of the hNS1 stem cells, which will be presented in the following sections. We wanted to fabricate a neurite guidance chip that allowed us to cultivate both cell lines without being negatively affected by the presumed factors mentioned above. Therefore, we focused on the production of chips where we could minimize the amount of PDMS and increase the media volume available to the cells.

## 2.1 Open Well Design

We started off by redesigning the chip into two 6 mm open squared wells, which were connected by the guidance grooves (see figure 5 a). The simplified basic structure made sure that the cells growing next to the grooves had enough cell media. Additionally, it had the great benefit of giving direct access to the cells, which for further detection analysis was very useful. SU-8 patterned Si-master contained grooves with a height of 4  $\mu\text{m}$  and two squared wells with a height of 200  $\mu\text{m}$ . We could not obtain higher functional layers with the SU-8 based master fabrication process. Therefore, the squared wells were cut/punched out manually after PDMS moulding to obtain the open wells. However, cutting the wells out manually precise enough was very difficult. It either led to an overhang of PDMS next to the grooves or it was cut into the grooves (see figure 5 b). When an overhang was present it was not possible to seed the cells close to the grooves, since most of them attached on top of the overhang. When cutting into the grooves we damaged the openings. Therefore, it was not possible to obtain sufficiently well defined grooves when using conventional PDMS soft lithography together with the open well design.

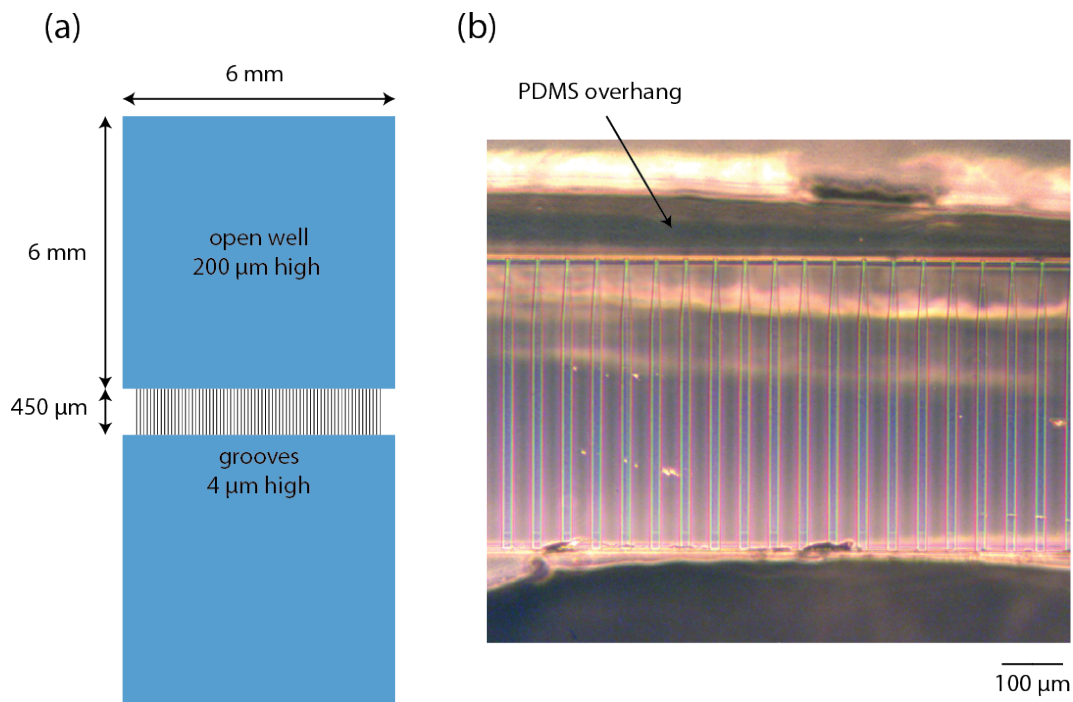
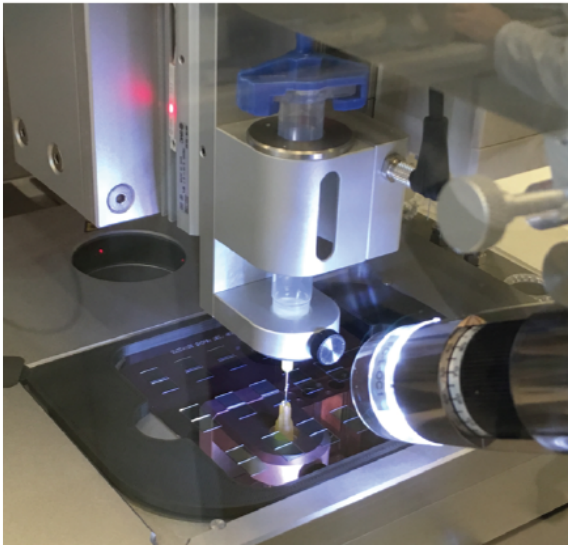


Figure 5: (a) Mask design of the open well chip consisting of two squared wells connected directly by the grooves (not in scale). (b) Image of the open well chip obtained by conventional replica moulding and manually punching out the wells. A PDMS overhang is visible on the top and on the bottom part, which hinders seeding cells directly next to the grooves.

## 2.2 3D Printed Soft Lithography

To fabricate an open well chip we needed a method that allowed us to deposit a well defined amount of PDMS onto the master mould. Sylgard 184 is mostly used for PDMS based microfluidic chip fabrication due to their easy application for replica moulding. However, since we needed to precisely deposit PDMS, it was not viscous enough and would have flown everywhere before being cured. Using more viscous PDMS it was possible to also 3D print PDMS [56]. Depositing PDMS with a 3D printer allowed us to deposit and create PDMS structures with much higher precision. The resolution of printing PDMS is not sufficient to form the neurite guidance grooves. Therefore, we used the novel approach of 3D printing PDMS onto a micro patterned Si-master (see figure 6 a). To the best of our knowledge such a method combining 3D printing and soft lithography has not been described in the literature yet.

(a)



(b)

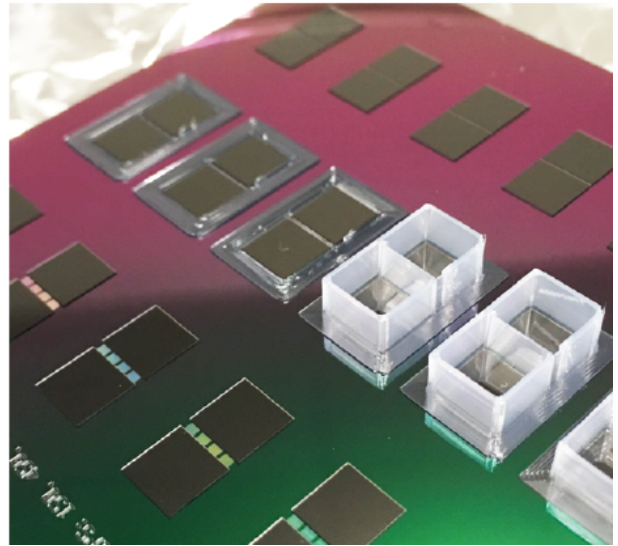


Figure 6: (a) Image of the 3D printer, depositing PDMS directly onto the Si-master mould. (b) Printed PDMS gasket and gaskets with printed shear thinning PDMS well extensions on top

PDMS was printed along the 6 mm squares and in between the gap on top of the neurite guidance grooves. Thanks to this, we were able to replicate precise structures in the millimetre scale (due to the 3D printer) as well as in the micrometre scale (due to micro patterned Si-master). However, to obtain a well defined 3D printed PDMS chip with imprinted guidance groove structure optimizations regarding the ink mixtures had to be performed

Mixing fumed silica beads with Sylgard 184 increased the viscosity. Adding adhesive PDMS SE1700 gave the ink shear-thinning properties. For the final printed chip, two different ink mixtures were used. Sylgard 184 containing 15% fumed silica beads and 20% SE1700 (further on referred as the gasket ink) was used to print the first 200  $\mu\text{m}$  high layer onto the master mould. The right ratio of silica beads and SE1700 to Sylgard 184 was needed for two main reasons. First, the viscosity needed to be high enough such that it was possible to print PDMS. Secondly, the amount of Sylgard 184 needed to be at a correct ratio that the ink still flowed slowly and filled out all the corners of the master mould. This was especially crucial to obtain well defined imprints of the guidance grooves. However, the gasket

ink was not shear-thinning enough to print the whole well structure on top. When the gasket ink was used to print higher above of the 200  $\mu\text{m}$  high SU-8 squares the ink would start to flow on top of the SU-8, which resulted in an overhang of PDMS. Therefore, a second ink mixture out of SE1700 containing 10% Sylgard 184 (further referred as the well ink) was used to print the roughly 5 mm high well extension structure on top. Due to the shear thinning properties, the well ink hardened quickly after being extruded through the printing nozzle. This made it possible to obtain well defined, thin and stable well extensions (see figure 6 b). The well ink itself could not be used to print the whole well structure directly onto the Si-master mould. The ink strongly attached to the SU-8 structures on the master after curing and in addition, it did not flow enough into all the small corners and thus did not fully replicate groove structure. With the combinations of the two described inks we managed to fabricate an open well PDMS based neurite guidance chip having well defined guidance grooves (see figure 7 a and b). It is worth mentioning that it was a crucial point that the well ink did not get in direct contact with SU-8. If it was the case due to small misalignment in the printing procedure, the printed gasket attached irreversibly to the SU-8. The specific pattern could then not be reused any more.

We would like to highlight that with this novel method it was possible to print much more complicated structures than just two squares onto a micro patterned master mould. Any shapes that can be drawn are possible. Obtaining different micro patterned PDMS shapes was not limited any more to the SU-8 patterns and the resolution obtained by manually cutting or punching. Dimensions that could not be achieved in such high precision by manually cutting PDMS but are too high for the SU-8 based master mould fabrication were now easily obtained. Therefore, we see great potential for the fabrication of many other microfluidic chips for a large variety of applications in 3D printed soft lithography.

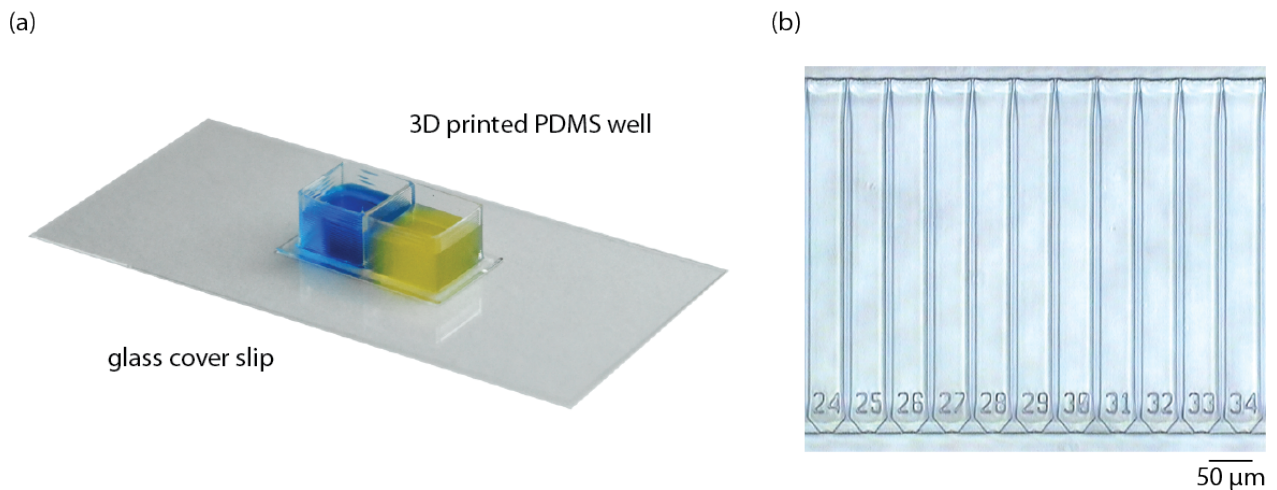


Figure 7: (a) Image of the 3D printed PDMS chip bonded onto a glass cover slip. (b) Guiding grooves from the 3D printed PDMS chip having well defined top and bottom edges.

### 2.3 Different Well-Extension Materials

To further minimize the amount of PDMS in the chip we tried to use different materials to extend the well instead of using the PDMS based well ink. Initially, we only printed a thin PDMS gasket (using the gasket ink) onto the Si master. Thereafter, instead of using the well ink to extend the wells we started off using 3D printed polylactide (PLA) as an alternative extension material. We constructed a clamp system where the gasket was clamped between a PLA well and the glass cover slip (see figure 8). The upper part and the bottom part of the clamps were tightened together by screws. Although this system worked for a short time, leaking problems occurred after the chips had been kept in the incubator for a few days. It was not possible to tighten the well structure completely, so that no leaking occurred without damaging the PDMS gasket or the cover slip. Additionally, PLA started to soak up culture media over time. Even when the structure was printed with 100% infill there were still small gaps in the structure and most likely due to capillary forces media was soaked up into the clamp.

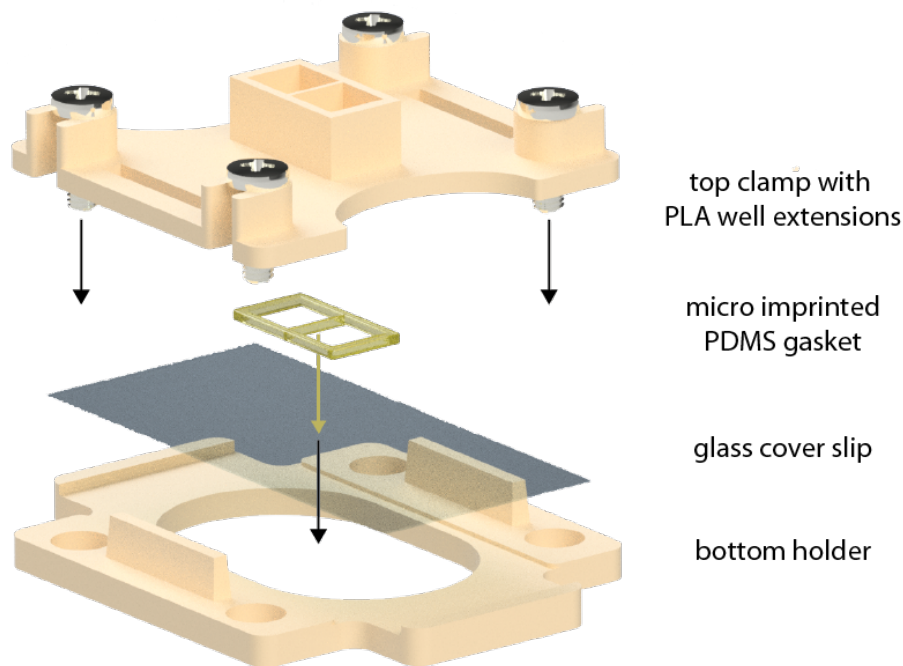


Figure 8: Graphical illustration of the 3D printed PLA clamp system by using a thin PDMS gasket. However, the clamp-chip set up started to soak up cell culture media and leaked after it had been kept in the cell incubator for a few days.

As a next approach we tried to glue PLA well extensions on top of the gaskets. To minimize the effect of PLA soaking up the culture media we wanted to obtain a well extension structure only consisting of single filament walls. PLA printing settings (extrusion width and printing speed) were optimized to obtain a  $350\ \mu\text{m}$  thin single filament wall. We then proceeded to glue the 5 mm high printed PLA well on top of the PDMS gasket.

The slightly round top surface of the PDMS gasket did not result in conformal contact between the

well extension and the gasket and made liquid-tight gluing impossible. Therefore, after printing the gasket three layers of well ink are printed to obtain a levelled surface. Because of the shear thinning properties we obtained a flat top surface, which allowed conformal contact between the well extension and the PDMS gasket.

We were then able to glue the well extension structure on top of the gasket using the following procedure. The well ink PDMS mixture was spin-coated on a blank Si-wafer to obtain a few micrometre thick layer. The PLA well was dipped in the spin-coated PDMS layer, aligned on top of the gasket and let to cure. Using the slightly viscous well ink and the described dipping method reassured that a consistent and minimal amount of PDMS was used to avoid excess PDMS flowing into the guidance grooves. By roughening the bottom part of the well structure using sandpaper before the gluing process we managed to additionally increase the bonding strength and decreased the chance of non-conformal gluing. An overview of the chip design and assembly is shown in figure 9.

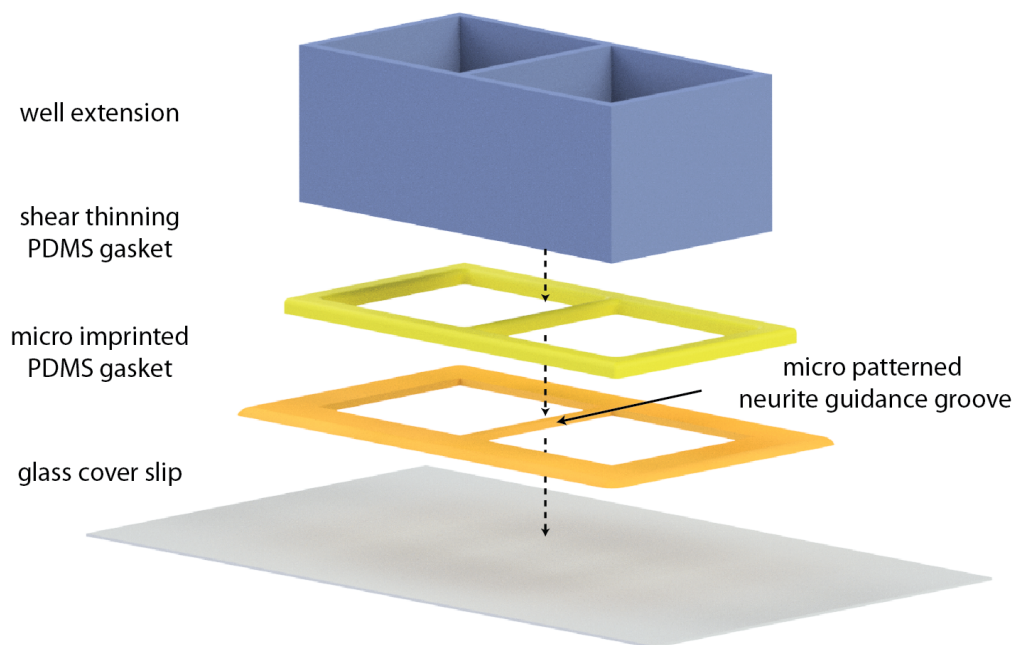


Figure 9: Graphical illustration of the gasket chip having PMMA or PLA well extensions. The chip consisted of the micro imprinted PDMS gasket having a shear thinning layer on top. Well extensions were then glued on top and the whole chip was bonded onto a glass cover slip.

The PLA-gasket chip did not leak when reversibly bonded on a glass cover slip. However, it was not possible to use PLA extensions when we wanted to covalently bond the chip onto glass using plasma activation. After plasma treatment PLA became very hydrophilic and the wells started to leak strongly since water was able to go in between the filament layers.

In order to have a chip that we could reversibly as well as covalently bond onto glass we needed to change the material for the well extension. We were able to fabricate the same well extension structure by micro milling into 5 mm thick PMMA sheets. We managed to glue the PMMA well extension onto

the gasket using the same procedure as for the PLA extension. Milling out the PMMA extensions took slightly longer than 3D printing them with PLA, but it enabled also fabrication with higher precision in regards to the thin wall between the two wells. Most importantly we were able to expose the PMMA-gasket chip to plasma and could bond it covalently onto glass, without inducing any leakage.

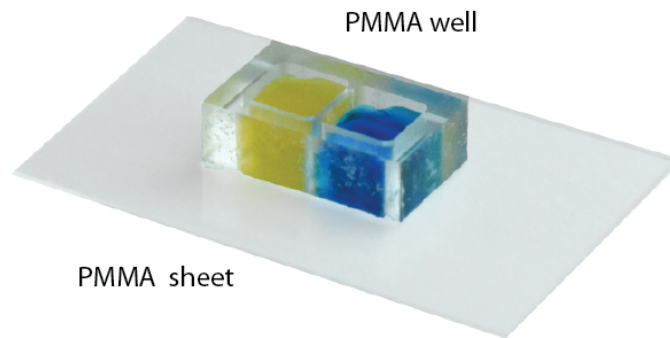
## 2.4 Hot Embossed PMMA Chip

In parallel to the gasket-chip approach where we minimized the amount of PDMS, we aimed to test a fabrication method where we could completely eliminate PDMS. If on a long run even after minimizing the PDMS, the hNS1 cells would still be negatively affected. We needed a fabrication method having sufficiently high resolution to obtain the neurite guidance grooves and allowed a certain flexibility in quickly varying the design of the grooves. Therefore, we were not left with too many options. From the literature we knew that it was possible to imprint microstructures into PMMA using SU-8 patterned Si-masters when correct temperature and pressure was applied.

We started off by micro milling 5 mm high well structures consisting of two milled out 6 mm squares that were connected by a 450  $\mu\text{m}$  wide gap. We then wanted to imprint the neurite guidance grooves into the PMMA between the two open wells. To do so we used a Si-master mould that contained the pattern of the guidance grooves and alignment marks. The milled PMMA well was manually aligned on top of the Si-master. We managed to optimize the temperature and pressure parameters ( $T = 105^\circ\text{C}$  and  $F = 2.1\text{ kN}$ ) to imprint the guidance grooves (see figure 10). Having the correct temperature was the crucial factor to obtain well defined imprints. When higher temperatures were applied, the PMMA started to melt and the well structure was squished under the pressure. Varying the pressure from 2.1 kN to 3 kN and the time from 60 s to 120 s did not change the outcome significantly. Compared to the PDMS-gasket chip the edges of the grooves were not as well defined. Additionally, since the alignment of the mould and the PMMA was done manually, the yield of well aligned grooves was rather low.

To bond the embossed PMMA well on a thin PMMA sheet, chemical welding was used. To do so 40%, 50%, 60% or 70% isopropanol (IPA) mixtures was added onto the PMMA sheet with a syringe. After IPA was added, two paper clamps were used to press the well onto the sheet and the chip was kept at  $65^\circ\text{C}$  for 1 hour. We wanted to see whether sufficiently strong bonding could be obtained without damaging the groove structures. We assumed that with higher concentration of IPA, the bonding strength increases, however, the chance of damaging/ dissolving the groove structure increases too. For the whole range of 40-70 % IPA sufficiently strong bonding was obtained so that the wells did not leak. However, also for the whole percentage range it occurred that the grooves were partly dissolved (see figure 10 a and b). Even though by trying different amounts and methods to add the IPA solution we did not manage to control the chemical bonding to a point where we could obtain a reasonable amount of bonded chips without damaged grooves. Chemical bonding has been reported to work well to bond PMMA-based microfluidic chips mostly for channels with higher depth. There the effect of IPA slightly dissolving the structures was not so significant. However, for shallow structures the process would need to be performed with a much higher precision when using IPA. Attempts in bonding the chips using hot pressing (applying only temperature and pressure) did not result in strong enough bonding and showed leaking problems.

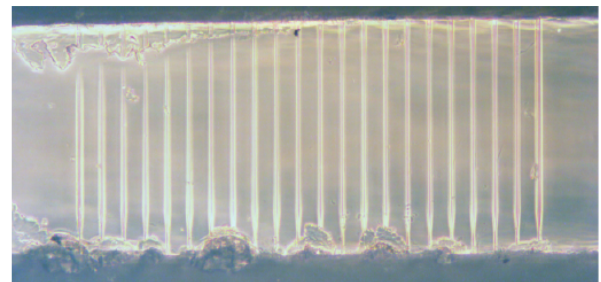
(a) hot embossed PMMA chip



(b) hot embossed grooves



before chemical bonding



after chemical bonding

200  $\mu\text{m}$

Figure 10: (a) Image of the PMMA based chip obtained by hot embossing and chemical welding. (b) Imprinted guidance groove in PMMA before and after bonding onto a PMMA sheet. After the chemical bonding the grooves were damaged.

Compared to the PDMS-gasket chip this approach does not contain any PDMS, however, the quality of the groove structure was significantly lower and the amount of chips that were damaged during fabrication process was much higher. The crucial point would be to find a better bonding strategy that would allow strong bonding without damaging the small groove structures. Additionally, the alignment of the wells with the master mould would need to be optimized in order to obtain precise groove imprints.

## 2.5 Discussion and Conclusion

Starting from the problem that the hNS1 cell line did not differentiate on the neurite guidance chip having closed PDMS channels but died within 2-3 days we launched a series of alternative fabrication approaches. We started out by introducing an open well design, to reassure the cells were exposed to sufficient cell culture media. Using conventional PDMS replica moulding it was not possible to obtain well defined guidance grooves together with 5 mm deep open wells. By using the novel combination of 3D printing PDMS onto the master mould, we were able to control the deposition of PDMS. After optimizing the inks, we managed to obtain printed PDMS chips consisting of two open wells connected by well defined imprinted guidance grooves. To further minimize the amount of PDMS in the chip we used the 3D printed PDMS gaskets, which contained the microgroove structure in combination with a PMMA well extension structure that we glued on top. That way we obtained a compartmentalized open well neurite guidance chip with minimized PDMS content. Additionally, using hot embossing we tried an alternative approach without using any PDMS. However, the quality of the obtained grooves was not sufficiently high.

From the long path in trying different approaches to obtain a microfluidic guidance chip that fulfils all our needs we manage to fabricate two open well design either with PDMS or PMMA well extensions. The open wells allow direct access to the cultivated cells, which simplifies further cell analysis methods. The minimized amount of PDMS allows cultivating cells that are sensitive to PDMS on a chip that could not be fabricated using other conventional materials. Lastly, the combination of 3D printing PDMS onto micro imprinted master mould would allow the fabrication of complex chip designs, with high precision on a micrometre scale and a millimetre scale. To the best of our knowledge no such fabrication method has previously been reported combining all those important features.

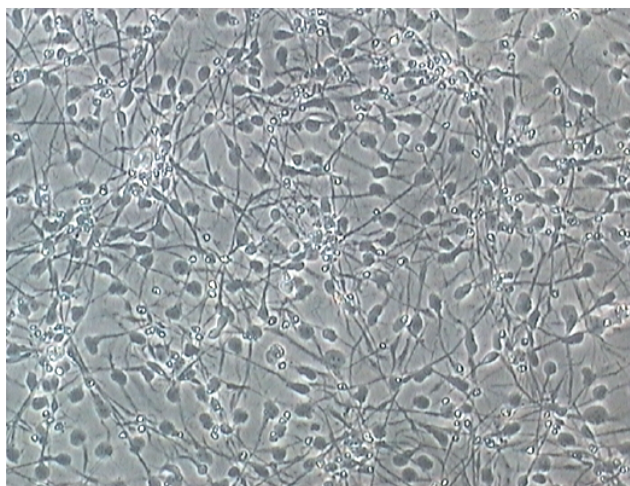
### 3 HNS1 Cell Viability Analysis

When we started differentiating the hNS1 cells on the first guidance chip having the closed channels, we could observe that the cells died within a few days. Therefore, we wanted to further understand if and how PDMS influences the cell viability. Additionally, after seeing that the presence of PDMS indeed did have a negative effect on the cells we wondered whether the negative effect could be eliminated. Therefore, we differentiated the hNS1 cells at different conditions exposing them to different amount of PDMS. The results will be presented and discussed in this chapter.

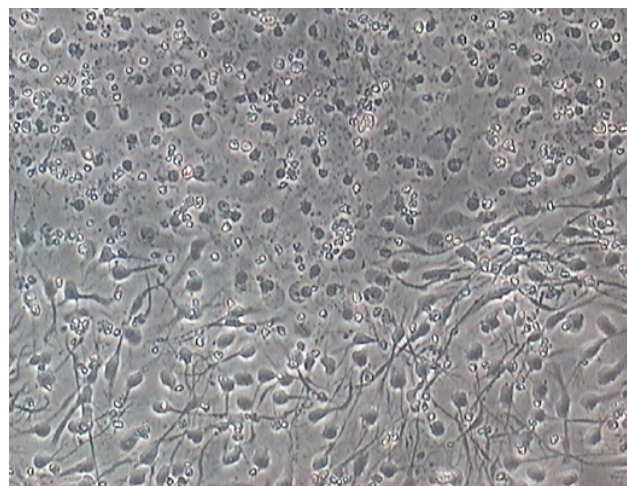
#### 3.1 PDMS Toxicity

To reassure that the cell death we saw was caused by PDMS, we compared cell differentiation of the hNS1 cells kept in normal differentiation media (DM) as well as in DM that was pre-incubated in round PDMS wells ( $\varnothing = 8$  mm). We observed that the forebrain cells kept in PDMS-DM all died within 15-20 days (see figure 11). The cell death due to PDMS was very distinct and easy to recognize under conventional bright field microscopy. No live/dead staining was needed to recognize the dead cells. They started to die from one (occasionally also two) spot. Cell death then spread out quickly and within 1-3 days all cells had died. Cells in control wells were cultivated up to 40 days without seeing such cell death. Based on information from the literature as discussed in the introduction we think that cell death is most likely caused by small non-crosslinked oligomers that leak out from PDMS over time or the uptake of hydrophobic molecules by PDMS. It could also be a combination of both effects. However, it became clear that PDMS had a negative effect on the hNS1 cells. No such drastic negative effect was seen on the differentiation process of the hVM1 cell line.

(a) control



(b) media exposed to PDMS



100  $\mu$ m

Figure 11: Bright field image of hNS1 cells after 12 days of differentiation on PLL coated well plates in (a) normal DM and (b) DM exposed to PDMS. It was visible how the hNS1 cells started dying and how cell death was spreading out through the well plate from one spot. The cells kept in media exposed to PDMS all died within the next two days, whereas in the control well the cells were unaffected and alive.

In a further step, we investigated the cell survival in different PDMS wells and chips. We measured how long the hNS1 cells survived in round PDMS wells having different diameters (6 mm and 8 mm) and different total amount of PDMS (thin wells and bulk wells) as well as on the different PDMS based neurite guidance chips (closed channel chip, 3D printed PDMS chip and PMMA-gasket chip) (see figure 12 a). We wanted to find out whether the total amount of PDMS or the PDMS surface exposed to the cell culture media is the important parameter influencing the cell viability. Additionally, we washed some PDMS chips intensively with different solvents to decrease the amount of non-crosslinked oligomers to see if this could also increase the cell viability. In figure 12 b it is shown how long the hNS1 cells survived in the corresponding well/ chip

The idea behind the washing procedure was that at the beginning solvents (hexane and ethylacetate) were used to swell the PDMS and thereafter less swelling solvents (acetone and water) were used to gradually wash out the prior used solvents together with non-crosslinked oligomers. After the washing procedure the PDMS wells had lost between 4-5% of their initial weight, meaning we successfully decreased the amount of some smaller oligomers. However, neither for the washed bulk wells nor for the washed thin wells, the cell viability changed significantly.

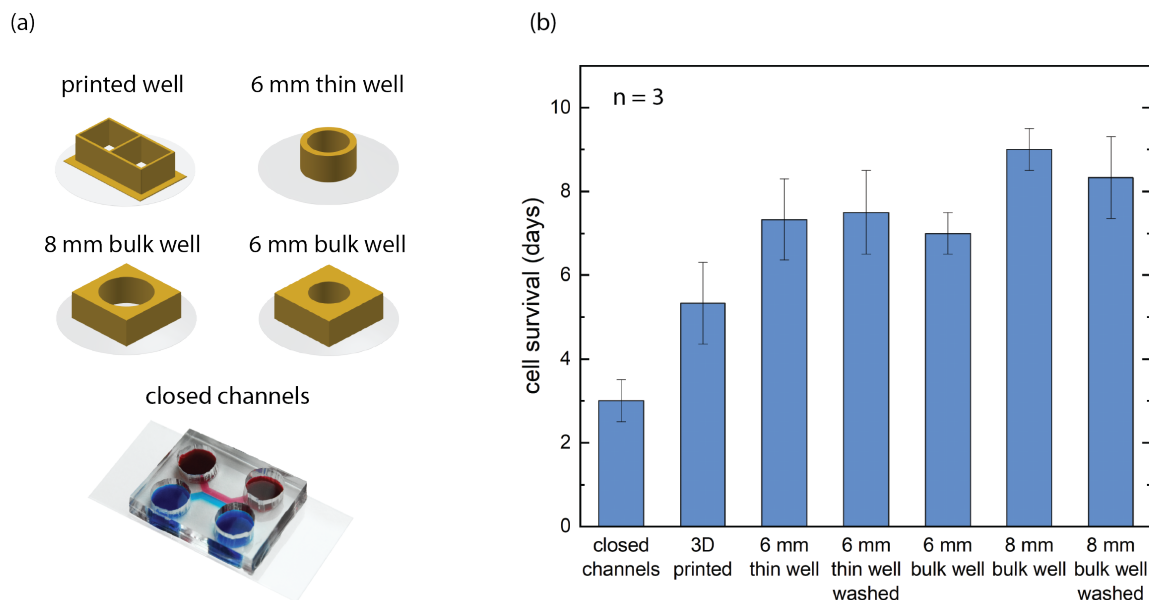


Figure 12: (a) Overview of the different PDMS wells and chips where hNS1 cell viability was tested. (b) Average hNS1 cell survival out of three experiments different with wells and chips. The cells died the fastest in the closed channel design. Washing procedures did not increase the cell viability. All wells were coated with geltrex.

In the closed channel chip, the cells died within 3 days. This was also the type of chip with the highest amount of PDMS compared to the relatively small media volume. However, by comparing the viability of the cells in the different type of wells and chips it became clear that the total amount of PDMS was not the primary negative factor. Otherwise the 6 mm bulk well would have shown a significantly different survival rate than the thin 6 mm well. Whether it was the uptake of hydrophobic molecules or the leaching out of non-crosslinked oligomers, the amount of cell media played an important role too. Therefore, we looked at the ratio of the cell culture media volume to the total PDMS volume as

well as the cell culture media volume to the PDMS surface exposed to cell culture media and compared those two ratios with the corresponding cell viability (see figure 13). A trend was visible that with a smaller surface area exposed to the culture media the cell viability increased. With the PMMA-gasket chip we managed to decrease this ratio so drastically that the PDMS toxicity effect was minimized and cells could survive even longer than 40 days. We can not fully exclude that for longer periods of time no negative effect will be observed. However, during the experiments we did not see any difference between the cells differentiated on the PMMA-gasket chip or in control well plates with no PDMS present.

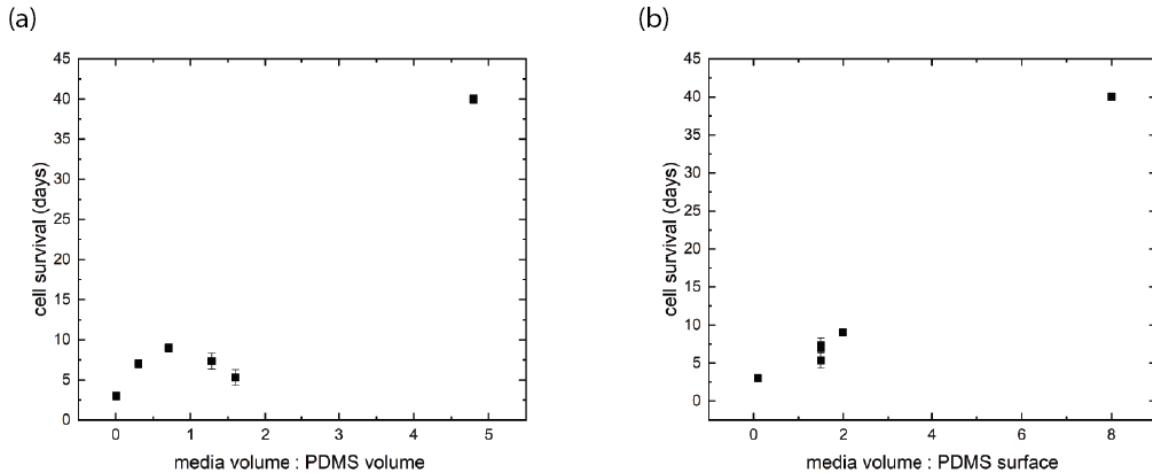


Figure 13: Cell survival of the different PDMS chips and wells plotted against (a) the media volume to PDMS volume ratio and (b) media volume to PDMS surface exposed to the culture media. It was visible that the amount of PDMS was not the critical factor but rather the PDMS surface exposed to the cell media. On the PMMA-gasket chip hNS1 cells were still alive after 40 days.

The same experiments were performed using Poly-L-Lysine (PLL) as well as geltrex coating. Geltrex is made out of extracellular matrix and compared to PLL coating it includes a mix of different proteins. When performing cell differentiation on geltrex this variety of proteins could influence the gene expression. PLL coating induces less unknown factors into the cell culture system and should therefore be preferred when working with stem cells. However, previous work in the lab showed that cell adhesion was better using geltrex. All cell experiments were therefore performed on PLL and geltrex coated surfaces. In this case, the cell viability only varied slightly and showed the same result concerning our conclusion that by minimizing the PDMS surface exposed to the culture media the toxicity effect decreased. For this reason, only the results using PLL coating are shown here.

We would like to point out that different PDMS curing times, lower and higher curing temperatures and different curing agent ratios from 1:5 to 1:10 have also been tested to see if this had an effect on the hNS1 cell viability. However, neither of those three parameters decrease the negative effect of PDMS on the cells.

### 3.2 Long-Term Differentiation of hNS1 Cells

With the PMMA-gasket chip, we managed to decrease the PDMS surface exposed to the cell media sufficiently that we could not see any toxic effects for hNS1 cells even after 40 days of differentiation on the chip. Since the cell differentiation protocol takes 10 days, this was long enough.

In figure 14, a confocal fluorescent image is shown, where calcein live staining has been performed after 30 days on-chip differentiation (hVM1 in orange-red and hNS1 in green). It was visible that both cell lines were still alive and showed neurite growth indicating the cells did differentiate. Unfortunately, the staining did not diffuse well into the grooves, which is why the fluorescent signal fades out and we needed to overexpose the image in order to see the neurites inside the grooves.

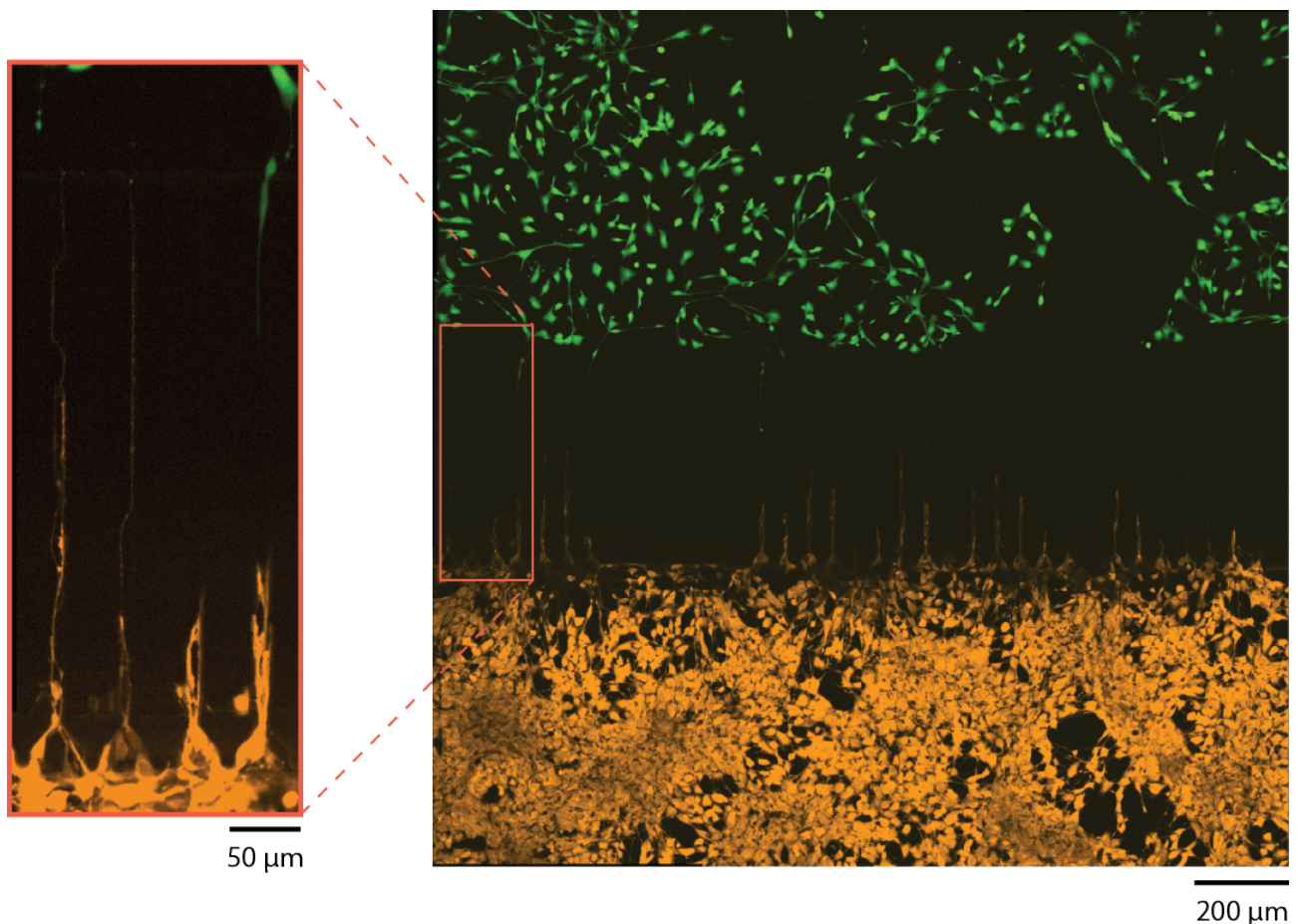


Figure 14: Live fluorescent stained image of hVM1 cells (bottom, in orange-red) and hNS1 cells (top, in green) after 30 days of differentiation on a PLL coated chip showed differentiated and alive cells. Due to poor diffusion of the live stain into the grooves, the grooves needed to be over exposed to visualize neurites growing through the grooves into the other compartment.

Further we wanted to see whether the cells differentiated into mature and healthy neurons that show spontaneous firing of action potentials. To measure this, calcium influx imaging was performed. The method allowed real time visualization of intracellular calcium concentration, which rapidly increases when an action potential is fired [57]. We incubated the differentiated cells with Fluo 3-AM, which changes from non-fluorescent into fluorescent state when binding to calcium ions. During the imaging process, cells were kept in a baseline buffer to be in a controlled ion concentration environment.

With a confocal spinning disk microscope we were able to record spontaneous action potential firing for some of the hNS1 cells after differentiated on-chip. Increase in fluorescent intensity progressing through the cells over time was seen (see figure 15). A fast increase followed by a slower (in some cases exponential) decrease was measured. This correlates with the expected calcium concentration after an action potential has been fired.

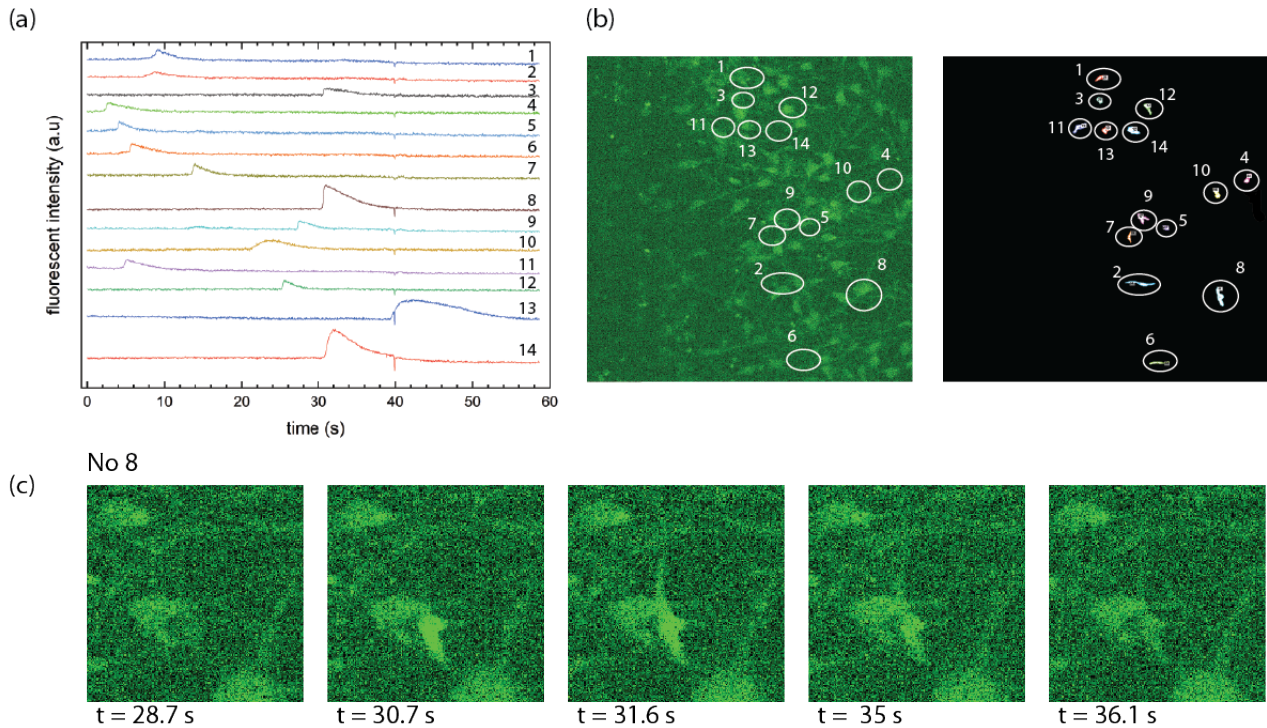


Figure 15: The illustrated results were obtained after performing calcium influx imaging on a geltrex coated chip after 17 days of differentiation. (a) The increase of the fluorescent signal indicated that a cell spontaneously fired an action potential. The average fluorescence progression over time of selected cells were marked in (b). (c) Zoomed in images of a selected cell showing the propagation of the action potential within the time frame of a few second.

### 3.3 Discussion and Conclusion

Previous work performed in the lab showed that PDMS had a toxic effect on hNS1 stem cell line. By analysing in more detailed how long the cells survived under different conditions we were able to demonstrate that it is indeed PDMS having a negative effect on the cells. We further found out that the important factor is how much PDMS surface is exposed to the cell culture media. In other words, the viability increased with a lower ratio of PDMS surface to the media volume. No other process such as washing, changes in curing time, and temperature had an observable effect on the cell viability. Only by reducing the PDMS surface in contact with the cell media the cells differentiated on the neurite guidance chips, without observing any visible toxic effect.

In the PMMA-gasket chip we cultivated the cells up to 40 days. Neurite growth was visible for both cell lines, indicating they did differentiate into neural cells. Additionally, we were able to observe spontaneous firing of action potential for the hNS1 cells indicating they differentiated into healthy and mature neurons.

## 4 Characterization of the two Cell Population

After successfully designing and fabricating a chip which allowed us to differentiate the two stem cell lines, we were able to start analysing the on-chip differentiation process. The aim, remodelling the nigrostriatal pathway means we wanted to have cells showing characteristics from the SNc on one side and on the other side cells showing characteristics from the striatum.

The most important characteristic of cells in the SNc is the presence of dopaminergic neurons. The on-chip differentiation of hVM1 cells into dopaminergic neurons was a crucial point. Just as important, the hNS1 cells should not differentiate into any dopaminergic cells at all. In figure 16 immunostained hVM1 and hNS1 cell are shown after 15 days on-chip differentiation on PLL as well as geltrex coated wells. TH antibodies showing red fluorescence signal indicated the presence of dopaminergic neurons in differentiated hVM1 cells on PLL and geltrex. No dopaminergic neurons were detected within the hNS1 cell population. Seeing that we only have dopaminergic neurons on one side of chip was a first step towards mimicking the nigrostriatal pathway

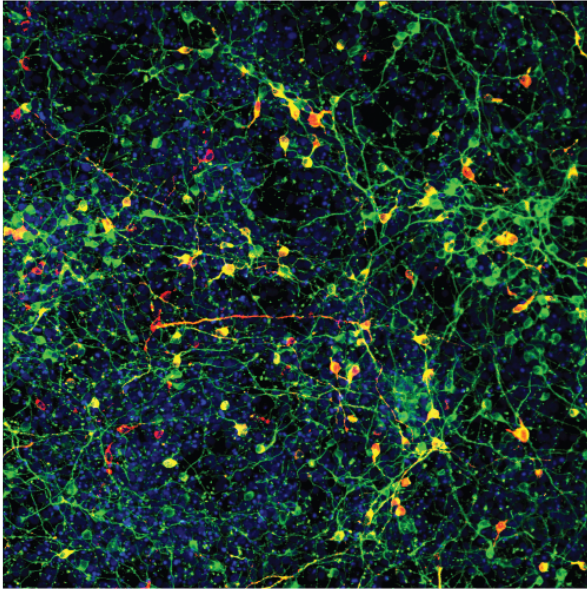
Looking at the TUBB3 staining (green fluorescence) it is visible that differentiated hNS1 cells show a different morphology on geltrex than on PLL. Axons on geltrex grew much longer compared to the axons on PLL.

In order to further characterize the hNS1 cells and compare them to the hVM1 cell line, immunostainings with anti GABA, GFAP, FOXG1 and DARPP32 were performed for on-chip differentiated cells. Anti GABA would mark GABAergic neurons. Anti GFAP indicated the presence of astrocytes. Anti FOXG1 could be used to identify neurons showing forebrain identity and anti DARPP32 to mark striatal neuron projections. All of the anti-bodies above mentioned were used in combination with anti MAP2 which is a marker for neuronal cells. The resulting images after immunostaining on geltrex coated chips are shown in figure 17. Similar results were obtained on PLL coated chips, which is why they are not additionally shown here. Neither hVM1 nor hNS1 differentiated into GABAergic neurons (figure 17 a). GABA is an inhibitory transmitter and mostly reduces neuronal excitability [58]. We did not expect to have any GABAergic neurons in our system. However, reassuring that our system did not contain any of them is useful to know in case experiments are performed where neurons are being excited. In such a case, GABAergic neurons could interfere with the performed measurements. Staining with anti-GFAP revealed that the hNS1 cell line mostly differentiated into astrocytes, whereas in the hVM1 cell line only few differentiated into astrocytes (figure 17 b). The high percentage of astrocytes in the differentiated cell population did match with results published when the cell line has been immortalized and the cell culture protocol has been established [59]. By looking at the staining results performed with anti FOXG1 we could observe staining of the hNS1 cell bodies, but we did not see such a strong and specific signal for the hVM1 cells (figure 17 c). FOXG1 is uniquely expressed in the embryonic forebrain and it is important for brain development [60]. This does indicate that the differentiated hNS1 cells did show forebrain characteristics. Unexpected and rather less than an ideal property for the targeted model was observed with the anti DARPP32 staining (figure 17 d). DARPP32 is part of one dopamine receptor signal transduction cascade and enriched in striatal neuron projections [61, 62]. No signal at all was detected in the hNS1 cells. However, in the hVM1 cell culture DARPP32 was present in some cells. By looking at the merged image showing MAP2 (green) and DARPP32 (red) it was visible that the largest amount of cells expressing DARPP32

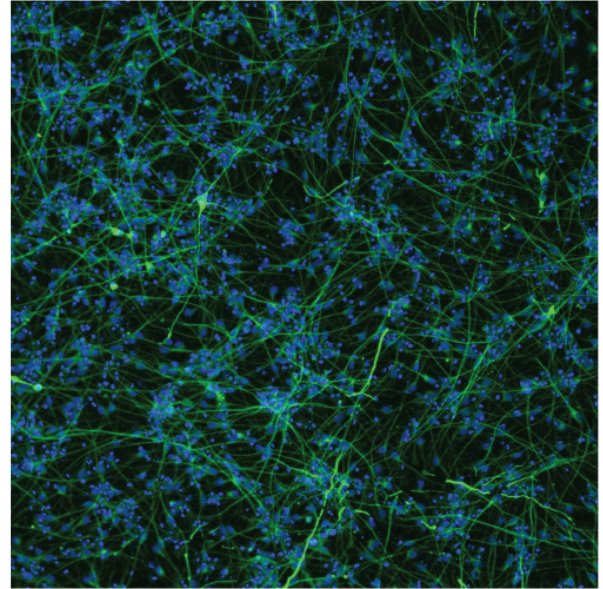
did not express MAP2 and vice versa. Therefore, it was possible to state that besides differentiating into dopaminergic as well as non-dopaminergic neural cells the hVM1 cell line also differentiates into non neuronal cells having dopamine receptors.

(a) geltrex coating

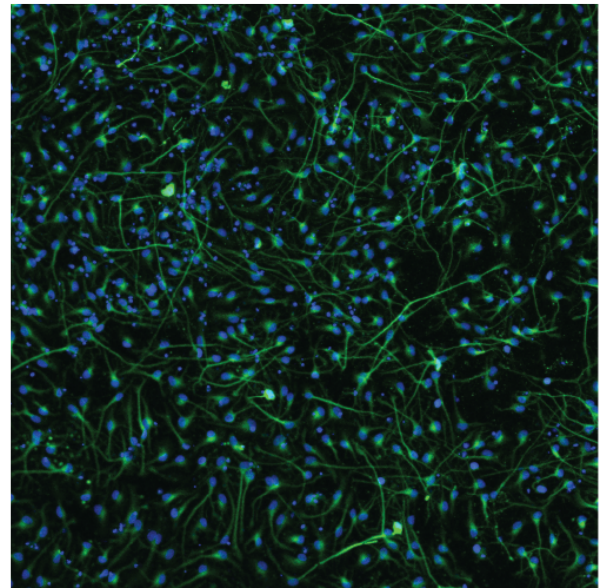
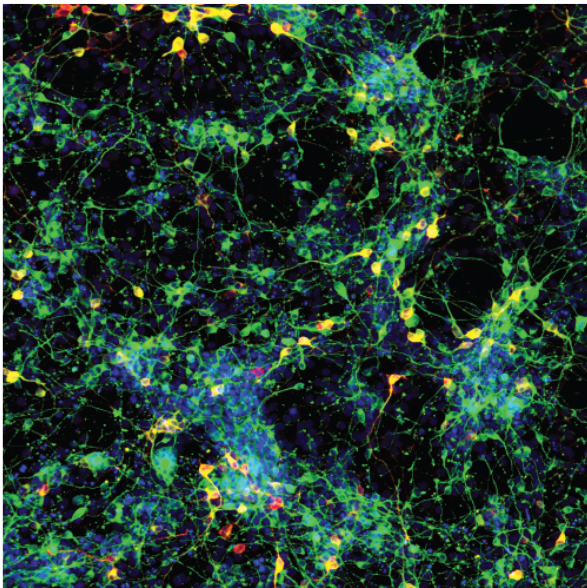
hVM1



hNS1



(b) PLL coating



TUBB3 / TH / Hoechst DNA

200  $\mu$ m

Figure 16: Immunostained fluorescent images of hVM1 and hNS1 cells after 15 days of differentiation on a (a) geltrex and (b) PLL coated chip. Anti-TH signal shown in red indicated the presence of dopaminergic neurons in the hVM1 side on geltrex and PLL coated surface. No dopaminergic cells were visible within the hNS1 cell population in the other compartment. Anti-TUBB3 staining showed the elongation of neurons in green and the nucleus of the cells stained using Hoechst were visible in blue.

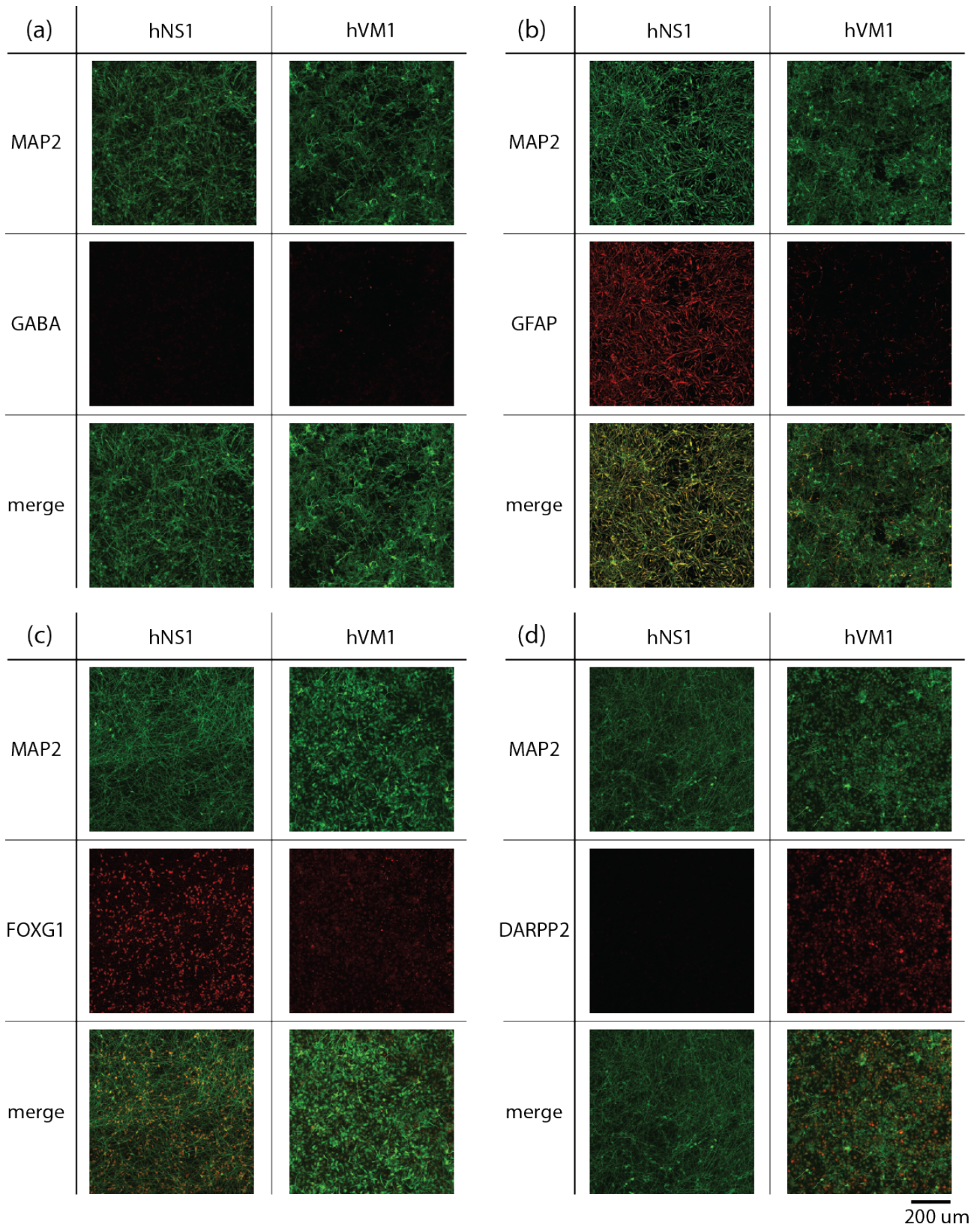


Figure 17: Fluorescent images of hNS1 and hVM1 cells on geltrex coated chips performed with anti-MAP2 showing the presence of microtubule structures and (a) anti-GABA, (b) anti-GFAP, (c) anti-FOXG1 and (d) anti-DARPP2.

Based on the performed Immunocytochemistry we were able to show that we managed to obtain dopaminergic cells only in the compartment representing SNc. No dopaminergic cells were found on the striatum side. The expression of FOXP1 within the hNS1 cell population assured that the striatum side had characteristics of the forebrain region. However, DARPP2 which is present in dopamine receiving neurons was not present in the hNS1 cell line at all. With the two cell lines it would be possible study dopamine release in the striatum compartment. To study in detail how the dopamine release reacts on striatal proteins containing dopamine receptors, another cell line would need to be incorporated. Since the PMMA-gasket chip has been optimized for sensitive neural stem cell, it is more likely that other cells can also be differentiated on the chip.

The high percentage of astrocytes in the hNS1 population would allow many further studies focusing on the impact of astrocytes in PD. Astrocytes are very abundant and have many important functions in the brain. Recent studies showed that many genes involved in PD are expressed in astrocytes and that their loss or miss function may be linked to PD [63, 64]. Here our model would serve well as a base to continue research on how specially astrocytes are involved in PD.

## 5 Reconstructing the Nigrostriatal Pathway

After we fabricated a neurite guidance chip where we could differentiate two stem cell lines and were able to show that they differentiated into cells having characteristics of the SNc as well as the striatum we had everything to start remodelling the nigrostriatal pathway. To do so we wanted to achieve directional neurite growth from the compartment containing the hVM1 cells to the compartment containing the hNS1 cells. Different groove designs were introduced to see whether the geometrical shape influences the neurite growth and were tested on geltrex and PLL coated chips

### 5.1 Seeding Optimization

The seeded cell concentration was a simple but very important factor, which influences cell growth and differentiation. We could observe on both coatings that hVM1 cells continued to proliferate when kept in the differentiation media where the growth factors (FGF and EGF) were absent. For that reason, fewer hVM1 cells than hNS1 cells were seeded in the chip. At low seeding concentrations on PLL coating the hVM1 cells did not differentiate well. Within a few days the cells started to form clumps causing spots without cells. Since we wanted to be sure to have cells close to the grooves a minimum seeding concentration of 70'000 cells/cm<sup>2</sup> was necessary. This effect was neither observed for hVM1 cells on geltrex coated chips nor hNS1 cells on geltrex or PLL coated chips. HNS1 cells were seeded at a concentration of 130'000 cells/cm<sup>2</sup>.

In order to obtain an evenly distributed layer of cells it was important to seed the cells in the exact volume of which one well could hold. If a smaller volume was used, the hydrophilic well caused a concave meniscus, which caused uneven seeding distribution across the well with higher cell density on the perimeter compared to if higher volume was used, a convex meniscus was formed which resulted in the opposite effect of having few cells next to the wall.

### 5.2 Microgroove for Directional Growth

To achieve directional guidance from one chip to the other we introduced a so called diode design. The basic idea was to have a “funnel“opening part on the hVM1 side to increase the chances of neurites entering the grooves, then having a narrow bottleneck that would minimize migration, having a wider middle part so that the neurites could grow all the way through, and at the end again a narrow opening that would prevent cell migration as well as decrease the chance that neurites would grow from the hNS1 side into the grooves. On one chip we incorporated four different designs to see whether one shape would increase one-directional neurite growth as well show a difference regarding cell migration (see figure 18 a). The four designs varied in the funnel opening size, the bottleneck width as well as the length of the bottleneck.

Figure 18 b shows all of the four different types of grooves on a geltrex coated chip after 14 days of differentiation. Anti TUBB3 labelling showed that for all four designs neurites grew through almost every groove. In some cases, even multiple neurites were present in a single groove. Similar results were obtained on different chips where cells had differentiated from 10 up to 20 days. The geometrical difference of the tested shapes was not enough to achieve a significant influence on guiding the neurites of the hVM1 and hNS1 stem cells. The amount of neurites growing through the grooves depended more whether the cells were evenly distributed in front of the grooves.

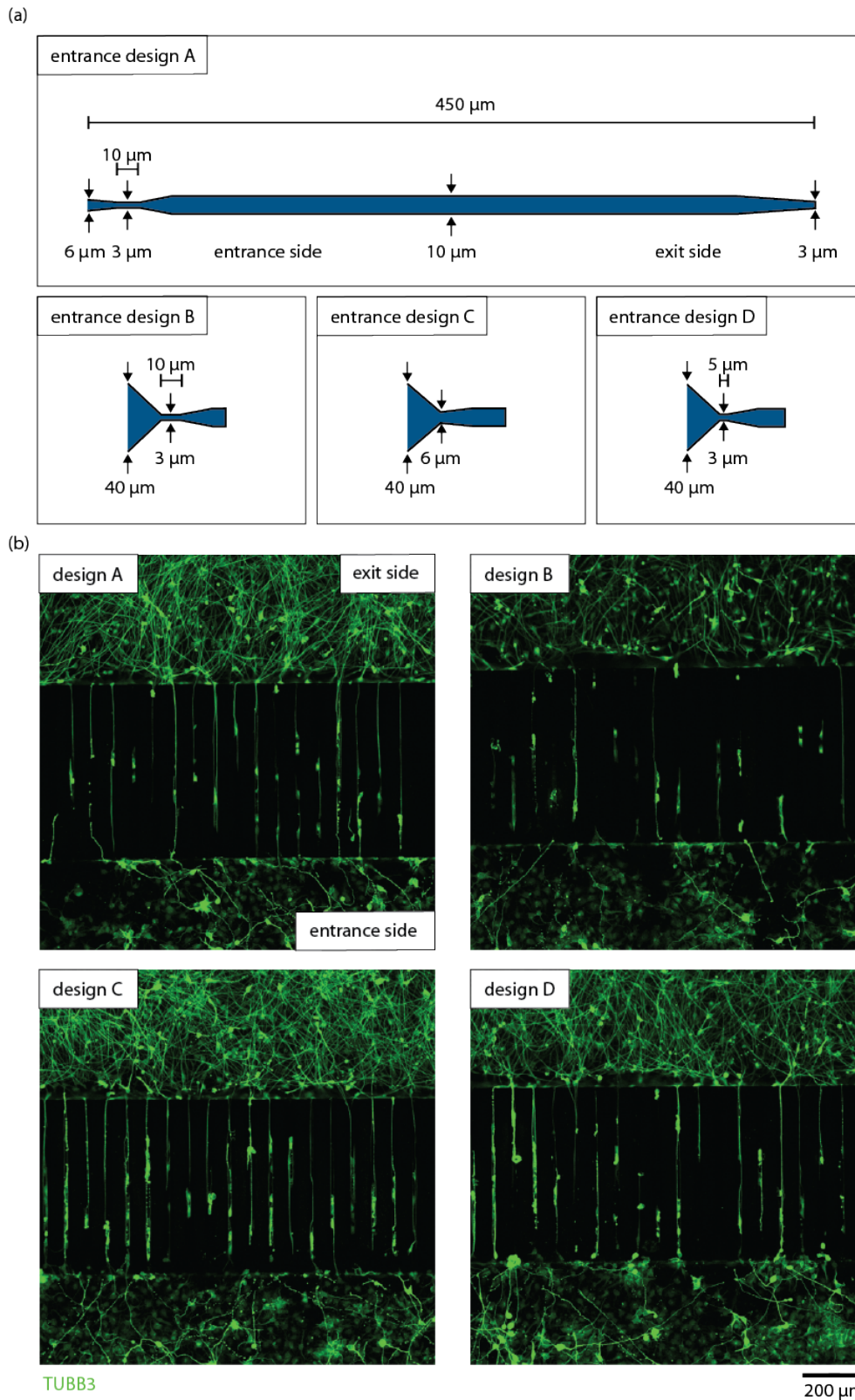


Figure 18: (a) Illustration showing the four different guidance groove openings which were present on one chip with which we wanted to influence one-directional neurite growth. (b) Fluorescent images of anti-TUBB3 stained cells after 15 days of differentiation on a geltrex coated chip. Neurites grew through all the different groove designs. The different geometrical shapes did not vary enough to see a difference in one-directional neurite growth.

It was also possible to see that cells on the hNS1 side grew into the grooves. However, due to the large amount of neurites, it was not possible to state whether the large opening on the hVM1 side significantly increased the chance of neurites growing into the grooves compared to the small opening on the hNS1 side. Studies where cells are only seeded on one side and/or where significantly less cells are seeded should be performed to obtain more data. As another modification we suggest to test an array of multiple funnel shaped geometries, towards the direction of the hNS1 compartment. Each funnel could decrease the chance that hNS1 cells would extend all the way through the grooves into the other compartment. Based on the established chip fabrication protocol changing the design of the grooves could be performed within a few days. Unfortunately, within the time of the project we did not manage to perform further cell differentiation experiments with the suggested design.

The narrow bottleneck was introduced into the design to stop cell migrating into the channels. Neither the length nor the width of it had a significant influence on stopping migration on geltrex coated chips. We did have some chips where the grooves were only 2  $\mu\text{m}$  high and even there migration was seen. However, a significant difference was visible in comparison to the PLL coated chips (see figure 19). By looking at the DNA stain (Hoechst stain in blue showing the nuclei) it is visible that migration into the grooves occurred very frequently on geltrex coated chips and much less on PLL coated chips.

It is important to point out that despite the low fluorescent signal in the grooves between the two wells one can clearly see that for both coatings neurites (labelled with anti TUBB3 in green) grew into the grooves. This indicates that the grooves on PLL were not blocked. It is remarkable that migration despite the small openings, migration on geltrex still occurs. Therefore, if one would like to decrease migration, PLL coating should be preferred.

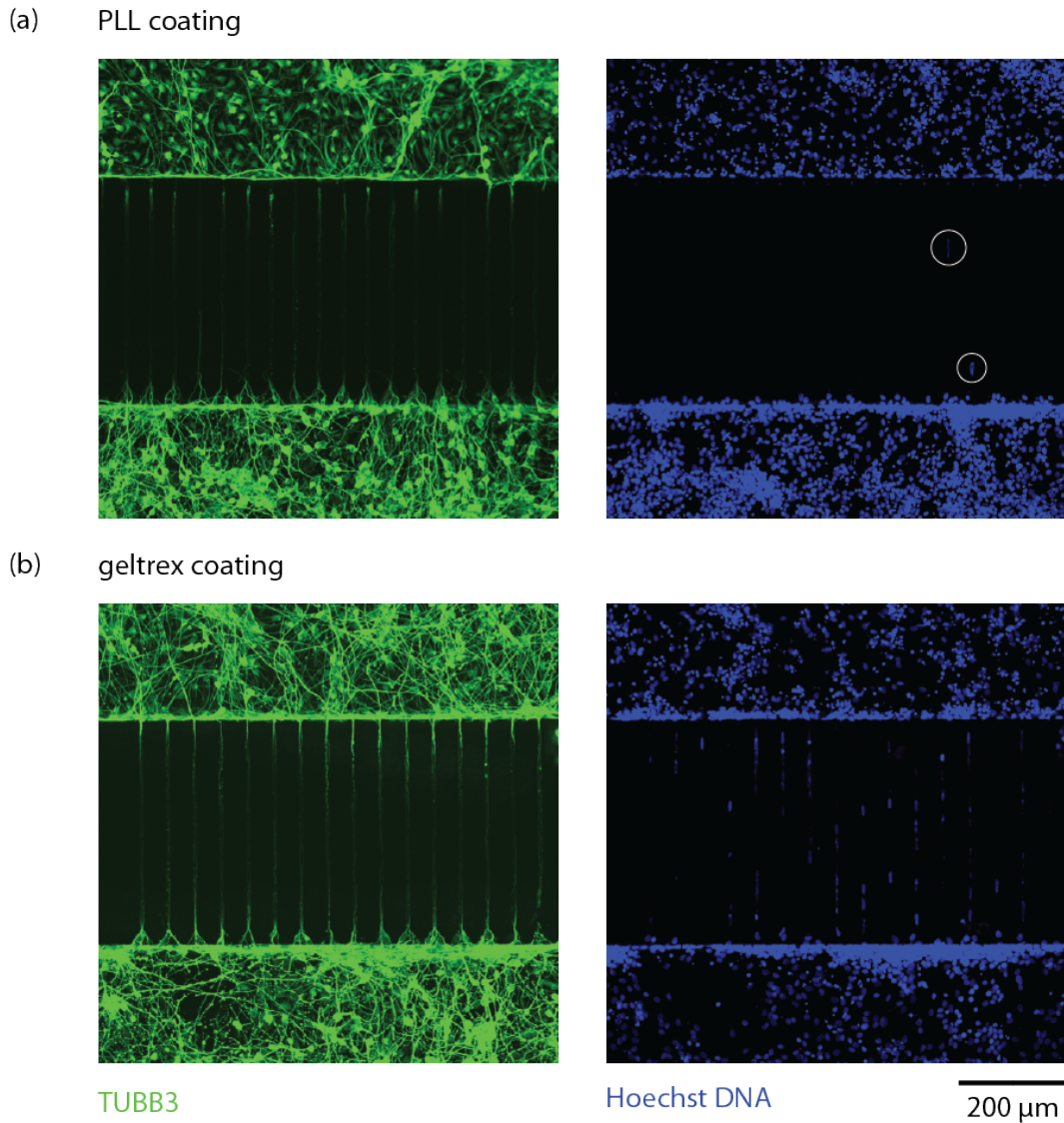
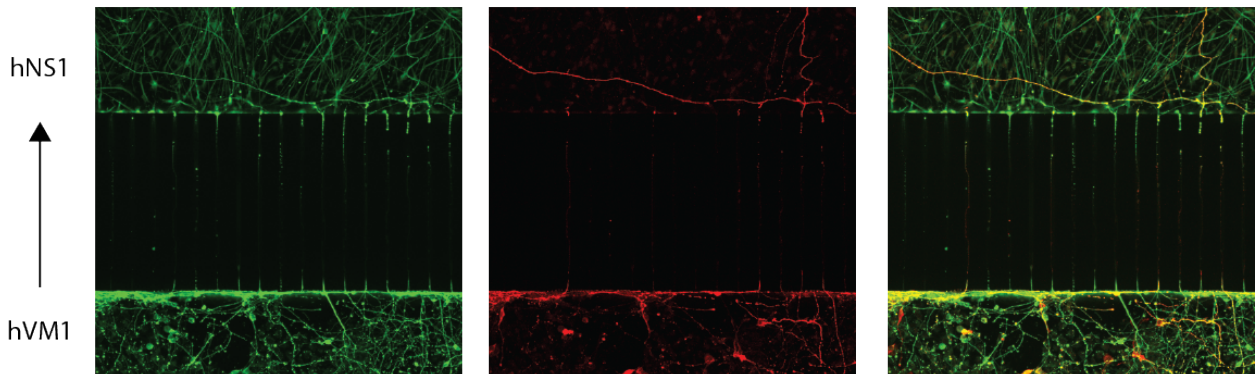


Figure 19: Fluorescent images after 10 and 11 days of differentiation on (a) PLL and (b) geltrex coated chips, respectively. HNS1 in the top and hVM1 cells in the bottom compartment, respectively. Anti-TUBB3 in green shows that neurites grew into the grooves on geltrex and PLL coated surface. However, cell migrated much more on the geltrex coated chip. The introduced bottleneck shape in the neurite groove design did not stop cells migrating into the grooves.

### 5.3 Nigrostriatal Pathway

Our final results of the approach to remodel the nigrostriatal pathway can be seen in figure 20. Fluorescent images after 20 and 16 days on-chip differentiation of hNS1 and hVM1 cells. In both chips we can see dopaminergic neurons (red fluorescent signal) entering the grooves from the compartment representing the substantia nigra (containing hVM1 cells) and exiting the grooves on the other side going into the compartment representing the striatum (containing hNS1 cells). Dopaminergic neurons having a length of up to one millimetre was observed. To differentiate cells into dopaminergic neurons and guide them in a separated compartment was indeed our primary goal.

(a) day 16 geltrex coated



(b) day 20 geltrex (hVM1) and PLL (hNS1) coated

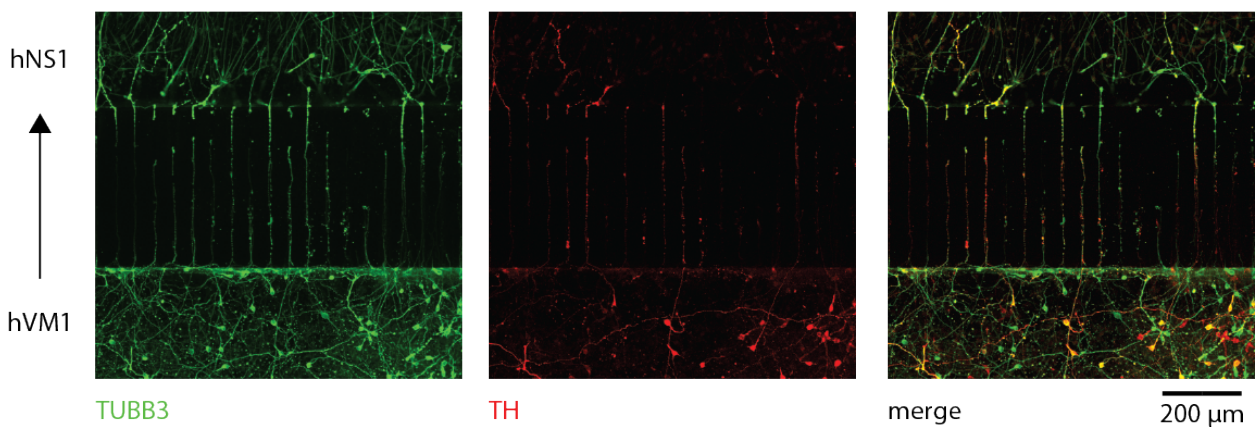


Figure 20: Fluorescent images of hNS1 and hVM1 cells after (a) 16 and (b) 20 days of differentiation. Anti-TH staining in red shows dopaminergic neurites growing into the grooves from the hVM1 side and out of the grooves into the hNS1 side, mimicking the nigrostriatal pathway. The weak fluorescent signal within the grooves is due to the poor diffusion of the antibodies into the grooves.

We could see that the concept of guiding dopaminergic neurons worked and managed to partly reconstructed the nigrostriatal pathway. With the introduced groove designs we did not manage to completely hinder hNS1 cells grow extensions into the grooves. Neither did the shape completely stop cells from migrating into the grooves. Migration was minimized when PLL coating was used.

After having developed a reliable fabrication method for our model further studies in regards to the neurite guidance could be performed to further minimize cell migration and analyse whether directional neurite growth can be achieved by changing the geometrical shape of the grooves.

Further analysis that could be performed is to measure dopamine concentration on the striatum side of the chip after chemical or electrical stimulation of the dopaminergic neurons on the SNc side. If an increase would be visible, we could show that dopaminergic neurons release dopamine through the grooves into the other side. It would also be interesting to see whether the neurons growing from the SNc compartment synaptically link with the hNS1 cells on the other side. A possibility to check this would be by performing retrograde tracing. Rabies virus or also pseudorabies virus can spread upstream through synaptically linked neurons and could be used to see whether they spread from the hNS1 cells to the hVM1 cell compartment.

## 6 Conclusion and Outlook

In the presented work we aimed to build a model mimicking the nigrostriatal pathway, which could help to better understand the complex development of PD and possible treatment strategies. Combining human stem cells with a neurite guidance microfluidic chip allowed us to create an *in vitro* human cell-based model exhibiting structural organisation. The basic neurite guidance chip design consists of two compartments which are connected by neurite guidance grooves. Existing neurite guidance chip fabrication methods do not allow to directly access the cells and use a high amount of PDMS.

The novel combination of soft lithography replica moulding with 3D printing of PDMS enabled us to fabricate PDMS based chips having high precision on a micrometre and millimetre scale simultaneously. With SU-8 based soft lithography replica moulding we were able to obtain an x-y resolution of three micrometres but were limited in the z resolution between 3-200  $\mu\text{m}$ . By printing PDMS onto a SU-8 micro patterned master mould we were able to deposit PDMS with a precision around 300  $\mu\text{m}$ . The combination of 3D printing PDMS with soft lithography replica moulding increased the resolution scale in x,y and z into the millimetre range.

We formulated two ink mixtures which allowed us to first print a layer of PDMS that imprinted the structure of the neurite guidance grooves and then add a second layer of shear-thinning ink to print stable PDMS extension structures on top. In combination with PMMA well extensions we obtained an open well neurite guidance chip with minimized amount of PDMS.

Cell viability studies showed that with decreased PDMS surface area exposed to cell media the viability increased. In the chip consisting of a thin PDMS gasket and PMMA well extensions the negative effect on the cell viability was not observed anymore. The chance of additional influences of PDMS which were not directly visible was also decreased.

After successfully fabricating a neurite guidance chip where we could differentiate two neural stem cell lines we were able to characterize the on-chip differentiated cells. The hVM1 cell line did differentiate into dopaminergic neurons, which is an important characteristic for the midbrain region. hNS1 cells representing the forebrain region were characterized by the presence of FOXG1, which is uniquely expressed in the embryonic forebrain. The presence of GFAP in the hNS1 cell line showed a high percentage of astrocytes.

By introducing a directional diode groove design, we wanted to induce one-directional neurite growth from one compartment to the other. The different tested geometrical shapes varied too little to see any improved one-directional growth within them. Gladkov *et al.* showed that asymmetric guiding channels had an influence on the neuronal growth by introducing an array of funnel shapes each increasing the chance of one-directional growth [31]. We assumed at the beginning that by adding to many funnel shapes we would completely hinder neurites growing through the channels. However, after seeing that our shapes did vary too little, an array of funnels should be tested. Cell migration into the grooves still occurred when having a 3  $\mu\text{m}$  thin bottleneck. As discussed by de Luca *et al.* stem cells have an inherent ability to migrate, which will most likely make it difficult for us to further minimize migration [65].

The microfluidic chip combined with the hVM1 and hNS1 stem cell lines resulted in a model showing important features of the nigrostriatal pathway in regard of the dopaminergic neurons growing into the cell line compartment which represented the forebrain region.

As discussed by Jou *et al.* and Booth *et al.* recent studies suggest that astrocytes contribute to the development of PD [63, 64]. Kostuk *et al.* exposed dopaminergic neurons to a PD mimetic toxin 1-methyl-4-phenylpyridinium and showed that the presence of astrocytes protected dopaminergic neurons from degeneration [66]. It would be very interesting to see whether the protection mechanism still functions when the astrocytes are only present around the dopaminergic projections and not in the same compartment as the dopaminergic neurons. With the presented model this could be further investigated.

The newly developed method of 3D printed replica moulding opens up many possibilities for microfluidic chip designs that before could not be fabricated. Complex geometries can be fabricated with high precision within a wide scale range. By fabricating a master mould as used for conventional replica moulding, a new chip design can be obtained within a few days, which is very useful for rapid prototyping. To the best of our knowledge no such method combining these advantages has been described before. We do see great potential in the 3D printed replica moulding for a wide application in microfluidic chip fabrication.

## 7 Materials and Methods

### 7.1 Soft Lithography

The concept of soft lithography was used to fabricate the neurite guidance chip. The two approaches: 1.) replica moulding and 2.) replica printing onto a master mould were performed to obtain a patterned layer of PDMS.

#### 7.1.1 Master Mould Fabrication

The mask for the Si-master was drawn in L-Edit v15.2. A total of 3 SU-8 layers were added to fabricate the master mould. SU-8 2005 negative resist was spin coated (60s, 5000 rpm) to target a 4  $\mu\text{m}$  thick resist layer which was used as an adhesive base layer to prevent small SU8 structures from peeling off. The wafer was soft baked for 3 minutes at 90° C, flood exposed to UV light (200mJ/cm<sup>2</sup>) for 16 minutes and post baked for 3 s at 90° C. The following day a second layer SU-8 2005 negative resist was spin coated (60s, 5000 rpm) to target a 4  $\mu\text{m}$  thick resist layer and soft baked for 3 minutes at 90° C. The wafer was exposed to UV for 16 minutes using a maskless aligner (210 mJ/cm<sup>2</sup>), post baked for 3 minutes at 90° C and developed using SU-8 developer for 30 s. This layer resulted in the few micrometer high groove structures. The following day, SU-8 2075 negative resist was spin coated (60 s, 1600 rpm) to target a 100  $\mu\text{m}$  thick third layer. The wafer was soft baked for 30 minutes at 90° C (ramped up within 10 minutes), exposed to UV through a glass mask (250 mJ/cm<sup>2</sup>), post baked for 5 minutes at 90° C and developed using SU-8 developer for 5 minutes. The last layer was performed to obtain the well structures which were connected by the thin groove structures.

The fabrication process to obtain the master mould was carried out in the clean room and was performed by Shashank Vasudevan.

#### 7.1.2 Conventional Replica Moulding

PDMS and curing agent (Dowsil 184 Silicone Elastomer Kit, Dow Europe GMBH, Germany) were mixed at a weight ratio of 10:1, degassed and stored in 50 mL Eppendorf tubes at -18° C for up to 1 month. Premixed PDMS was left to warm up to room temperature (RT), poured onto the master mould and hardened at 60° C over night. The approximately 5 mm PDMS thick layer was peeled off and chips were cut and punched using a disposable scalpel (Swann-Morton, England) and a 6 or 8 mm biopsy punch (Pelomi, Denmark), respectively.

#### 7.1.3 3D Printed Replica Moulding

A 3D-Discovery Printer (regenHU, Switzerland) was used to print PDMS on top of the master mould. Two Ink mixtures out of Dowsil SE 1700 clear base (Dow Europe GMBH, Wiesbaden Germany), Sylgard 184 (Sigma-Aldrich, Germany) and fumed silica beads (0.2-0.3  $\mu\text{m}$ , Sigma-Aldrich, Germany) were used for printing. The first ink (gasket ink) contained Sylgard 184 with 15% fumed silica beads and 20% SE1700 and was used to print onto the micro patterned Si-master mould. The second ink (well ink) mixed out of SE1700 with 10% Sylgard 184 was used to print structures on top of the well ink. PDMS was printed using a pneumatic extruder through a plastic conical needle with a diameter of 200  $\mu\text{m}$ . Printed PDMS was cured at 60° C over night before peeled off from the wafer. PDMS printing was performed by Janko Kajtez.

## 7.2 PLA Printing

3D printed parts were modelled using Autodesk Inventor Professional 2019. Simplify 3D 4.0.1 software was used to generate the g-code. In order to print a single extrusion wall with a thickness of 350  $\mu\text{m}$  a few adaptations were made from the standard settings of the Sliceprofile Simplify 3D-FELIX Pro Series Extreme Quality (50  $\mu\text{m}$ ). Extrusion width was set to 0.25 mm, first layer height 200%, first layer width 150%, first layer speed 50%, default printing speed 1500 mm/min, axis movement speed x/y 3000 and z 1000 mm/min and single extrusion walls as well as single extrusion fills were allowed. The structures were printed with a FELIX Pro 2 printer (Felix Printers, Netherlands) and PLA filament (PLA White 1.75 mm, Innofil3D, Netherlands)

## 7.3 Micromilling

Micromilled structures were drawn with Autodesk Inventor Professional 2019. Cimatron E 12.0 was used to generate the g-code for the milling machine (Mini-Mill/3PRO, Minitech Machinery Corp., USA). Milling was performed using a 1.5 mm solid endmill (2F ext reach, Japan) at a rotation speed of 8000 rpm into a 5 mm thick PMMA sheet (Evonik Röhm GmbH, Germany). In order to avoid that the milling tool touches the double sided tape on the bottom side of the PMMA sheet, the parameters were set that only a thickness of 4.8 mm was milled out. The remaining thin layer was then broken off manually. This prevented that small irremovable parts of the tape were stuck to the milled structure.

## 7.4 Hot Embossing

Hot embossing was performed using a Collin Press 300 SV (COLLIN Lab and Pilot Solutions GmbH, Germany). Micromilled PMMA wells were hot embossed with a SU8 patterned Si-master mould. Using the automatic mode, a two step program was used (see table 1). The first step was applied to imprint the microstructure and the second step to cool down the PMMA before the demoulding.

Table 1: A two step automatic program was used with the indicated parameters

Step No.	Force	Temperature	Time	cooling constant
1	2.1 kN	105	120 s	-
2	2.1 kN	50	205	20 K/min

## 7.5 Chip Assembly

### *PDMS Chips*

The basic assembly for all PDMS based chips and wells was performed as followed. Cover glasses were incubated over night in 96 % Ethanol (VWR International S.A.S, France) and washed with sterile-filtered cell culture water (Sigma-Aldrich, Germany). Cut out and/ or punched chips were either reversibly or covalently bonded to a cover glass. For covalent bonding, PDMS chips and the cover glasses were exposed to air plasma at 0.8 mbar for 45 s. The bonded chips were then put in the oven or on a hot plate at 65° C for 20 minutes. To sterilize, 0.5 mM NaOH (Sigma-Aldrich, Germany) was added into the wells, incubated for 20 minutes and washed three times with phosphate buffered saline (PBS). For chips containing guidance grooves, adding NaOH was performed within 1 hour after plasma treatment to make sure the PDMS surface was still hydrophilic and the grooves were wetted

properly. No plasma activation was used for reversible bonding. To wet the grooves in reversible bonded chips, 96 % ethanol was added for 5 minutes and washed 3 times with PBS. For additional sterilization, all chips were put under UV light for 20 minutes. Chips were then coated either with 100x diluted geltrex (ThermoFischer Scientific, USA) or 30  $\mu\text{g}/\text{mL}$  PLL (Sigma Aldrich, Germany) over night at 37° C. PLL coated chips were washed three times with PBS before cell seeding.

Additional steps before bonding onto glass cover slips were performed for the gasket chip having PLA or PMMA well extensions. The bottom surface of the PLA/PMMA-well structure was roughened using sandpaper (p400), dipped onto a spin coated layer of the PDMS well ink (4 min. 2000 rpm with 300 rpm/s acceleration) for 10 s and placed on top of the PDMS gasket with the help of an optical microscope. To cure the PDMS glue, the chips were kept in the oven over night at 60° C. The chips were then bonded on glass as described above.

#### *Hot embossed chips*

PMMA well structures were micro milled as described in section 7.3. The structure consisted of two 6 mm x 6 mm wells with a distance of 450  $\mu\text{m}$  in between. The Well structures were then manually aligned onto a Si-master containing negative imprints of 4  $\mu\text{m}$  high neurite guidance grooves. By using hot embossing as described in section 7.4, the grooves were imprinted into the PMMA between the two wells. The embossed wells were then bonded onto a 0.5 mm thin PMMA sheet using chemical welding. PMMA was pre washed with detergent and rinsed several times with milli-Q water. A thin layer of 40, 50, 60 or 70 % IPA in water was put on top of the PMMA sheet. To do so, the two PMMA pieces were pressed together using two conventional paper clamps and put into the oven at 65° C for 1 hour. The bonded chips were then sterilized and coated as performed for the PDMS chips.

## **7.6 PDMS Washing Procedure**

When PDMS was washed to extract non-crosslinked oligomers the following washing protocol was performed. Cured and cut PDMS chips/wells were incubated in 45 ml hexane (2 x 12 h), 45 mL ethylacetate (2 x 12 h) and acetone (2 x 24 h). The PDMS was then dried in the oven at 60° C for 48 hours and then washed again in cell culture tested water (2 x 24 h).

## **7.7 Cell Culture**

#### *Cell Lines:*

Two human neural stem cell lines were used, human neural stem cell line 1 (hNS1) and human ventral mesencephalic neural stem cell line (hVM1) BcL-X<sub>L</sub> (basal cell lymphoma-extra large) stem cells.

HNS1 cell were derived from the diencephalic and telencephalic (forebrain regions) of a 10-10.5 week old aborted human embryo. The cells were immortalized by infection with a retroviral vector coding for *v-myc* (the p100 gag-myc fusion protein isolated from avian virus genome). Establishment of the hNS1 cell line is described in detail by Villa *et al.* [59].

HVM1 BcL-X<sub>L</sub> were isolated from a 10 week old aborted human fetus and immortalized using *v-myc*. hVM1 cell line was infected at passage 6 with BcL-X<sub>L</sub>, which enhances differentiation into dopaminergic neurons. Detail protocols of the immortalisation as well as the BcL-X<sub>L</sub> overexpression were published by Villa *et al.* and Courtois *et al.*, respectively [36, 67].

*Reagents for Cell culture and differentiation:*

Dulbecco's Modified Eagle Medium/Nutrient Mixture F-12 (DMEM/F12 ), AlbuMax I, 1M N-2-hydroxyethylpiperazine-N-2-ethane sulfonic acid (HEPES) buffer, N-2 supplement and Geltrex was purchased from ThermoFischer. Glucose (BioReagent), penicillin streptomycin (P/s), Poly-L-Lysin (PLL) and Bucladesine sodium salt (db-cAMP) were purchased from Sigma Aldrich. TrypLE was purchased from gibco. L-alanine, L-asparagine monohydrate, L-aspartic acid, L-glutamic acid and L-proline were purchased from MerckMillipore. Non-essential aminoacids (NEAA mix) were mixed in the quantities as shown in table 2 with warm water under stirring, filter sterilised and stored at -20° C.

Table 2: Recipe for preparing NEAA mix

<b>Aminoacid</b>	<b>For 100 mL NEAA mix [mg]</b>
L-alanine	356
L-asparagine·H <sub>2</sub> O	600
L-aspartic acid	531
L-glutamic acid	588
L-proline	460

Recombinant Human epidermal growth factor Protein (EGF) and Recombinant Human fibroblast growth factor basic (146 aa) Protein (FGF) were purchased from R&D Systems. Glial-Derived Neurotrophic Factor (GDNF) was purchases from PeproTech.

*Media Preparation:*

For the basic media (BM) 3 g of glucose, 2.5 g AlbuMax I and 2.5 mL HEPES were mixed with 500 mL DMEM/F12 and filter sterilised. BM was stored at 4° C up to one month.

For the growth media (GM) 500  $\mu$ L of P/S 100x, 500  $\mu$ L N-2 supplement, 500  $\mu$ L NEAA mix, 10  $\mu$ L EGF (100  $\mu$ g/ mL in PBS) and 50  $\mu$ L FGF (20  $\mu$ g/mL in PBS containing 0.1 % BSA) were mixed with 48.5 mL with BM.

For the differentiation media (DM) 500  $\mu$ L of P/S 100x, 500  $\mu$ L N-2 supplement, 500  $\mu$ L NEAA mix, 500  $\mu$ L db-cAMP (50 mg/mL in cell tested water) and 10  $\mu$ L GDNF (2 $\mu$ g/mL) were mixed with 48 mL BM.

*Flask coating:*

Cells were cultured on geltrex or PLL coated T25 flasks. For PLL coating, flasks were incubated over night with 3 mL of 10  $\mu$ g/mL PLL at 37° C, washed 3 times with PBS and left to dry. Dry flasks were stored at -18° C and washed once with PBS before cells were seeded. For geltrex coating, 1.5 mL of 100x diluted geltrex was added into the flask and left over night at 37° C. Geltrex coating was removed prior to cell seeding

*Growing cells and passing cells:*

Cells were kept in the incubator at 37° C containing 5% of CO<sub>2</sub>. When the cells were 80% confluent they were passed into a new flask for further cultivation or onto the chips to start differentiation.

To do so the following steps were performed. BM, GM, PBS were pre-warmed in the water bath at 37° C and TrypLE was let to warm up to RT. GM was removed from the culture flask and 3 mL of warm PBS was added to rinse the surface. After PBS had been removed, 1 mL of TrypLE was added. The flask was incubated at 37° C for 5 minutes for the cells to detach. Then 3 mL of BM was added to deactivate the TrypLE. The BM containing the cells was transferred into a 15 mL falcon tube and centrifuged for 5 minutes at 200 G. After the cell suspension had been centrifuged, the supernatant was removed and the cells were resuspended in 3 mL of warm GM. The desired amount of cells was then added to a new flask.

#### *Cell Differentiation:*

Cells were seeded onto the desired surface at the desired density after performing the cell passing step described above. After 24 hours all GM was removed and warm DM was added. After additional 24 hours all DM was replaced by new warm DM. Thereafter, every second day 2/3 of the DM was replaced by new warm DM until the end of the desired differentiation. Cells were kept in the incubator 37° C containing 5% of CO<sub>2</sub>.

## **7.8 Immunocytochemistry**

#### *Reagents for Staining:*

Fixation buffer was purchased from life technologies. Goat serum (GS), horse serum (HS), Triton X-100 (Tx), anti- $\beta$ -Tubulin III antibody (anti-TUBB2) produced in mouse, anti-GABA antibody produced in rabbit, calcein acetoxymethyl ester (calcein-AM), magnesium chloride (MgCl<sub>2</sub>), calcium chloride (CaCl<sub>2</sub>), sodium chloride (NaCl) and potassium chloride (KCl) were purchased from Sigma Aldrich. Anti-tyrosine hydroxylase antibody (anti-TH) produced in rabbit was purchased from Pel Freez. Calcein red-orange AM and fluo-3 AM were purchased from Thermo Fischer Scientific. Anti-(rabbit)-[647] and anti-(mouse)-[546] was purchased from Life Tech. Anti-FOXG1 antibody produced in rabbit, anti-DARPP32 antibody produced in rabbit and anti-MAP2 antibody produced in chicken were purchased from abcam. Cy2 affiniPure Dokey anti-rabbit and Cy5 affiniPure Donkey anti-chicken were purchased from Jackson Immuno Research. Anti-GFAP antibody produced in rabbit was purchased from DAKO. PBS used for staining was purchased from gibco.

#### *Live Staining:*

Live staining was performed using calcein-AM and calcein red orange AM together with Hoechst stain. Cells were incubated in BM containing 2  $\mu$ g/mL calcein and 20  $\mu$ g/mL Hoechst for 20 minutes at 37° C and washed once with BM before imaging.

#### *Fixing Cells:*

For fixation the cells were washed with PBS and incubated for 5 minutes at 37° C, incubated for 15 minutes with fixation buffer at RT and then washed 3 times with PBS

#### *Immunostaining:*

Cells were washed twice with PBS containing 0.3% Tx. To block unspecific binding cells were incubated for 1 hour at RT in PBS containing 0.3% Tx, 5% GS and 5% HS. Primary antibodies

were added in PBS containing 0.3% tx, 1% GS and 1% HS and left overnight at 4° C. Before adding the secondary antibodies, cells were washed 3 times with PBS-Tx. Corresponding Secondary antibodies were added in BPS-Tx containing 1% GS and 1% HS and left overnight at 4° C. Cells were washed three times with PBS-Tx before incubated for 20 minutes with  $\mu\text{g}/\text{mL}$  Hoechst stain DNA stain in PBS-Tx. Cells were then washed again three times before being imaged. The used primary and the corresponding secondary antibodies as well as their concentrations are shown in table 3

Table 3: List of used primary and corresponding secondary antibodies.

<b>Primary Antibody</b>	<b>Secondary Antibody</b>	<b>Dilution</b>
anti-TH (rabbit)	anti-(rabbit)-[647]	1:500
anti-TUBB3 (mouse)	anti-(mouse)-[546]	1:500
anti-GABA (rabbit)	Cy2 anti-(rabbit)	1:1000
anti-GFAP (rabbit)	Cy2 anti-(rabbit)	1:1000
anti-FOXP1 (rabbit)	Cy2 anti-(rabbit)	1:1000
anti-DARP32 (rabbit)	Cy2 anti-(rabbit)	1:1000
anti-MAP2 (chicken)	Cy5 anti-(chicken)	1:1000

*Calcium influx imaging:*

Cells were incubated in BM having a concentration of 3 mM Fluo-3 AM for 30 minutes at 37° C and then washed once with BM. Before imaging cells were washed once with a baseline buffer (1.2 mM  $\text{MgCl}_2$ , 2mM  $\text{CaCl}_2$ , 150 mM NaCl, 5 mM KCl, 5mM glucose and 10 mM HEPES) and then kept in the baseline buffer during imaging.

### 7.9 Optical and Fluorescent Imaging and Image Analysis

Fluorescent microscopy was performed using a confocal laser scanning microscope (LSM) T-pmt 710 on an inverted axio observer from Zeiss or an inverted nikon Ti2 with a yokogawa CSU-W1 SD system (50  $\mu\text{m}$  pinholes). Fluorescent intensity was evaluated using ImageJ 2.0.0. Optical images were taken using an inverted primovert from Zeiss

## 8 References

- [1] James Parkinson. An essay on the shaking palsy. *Shweood, Neely and Jones*, 1817.
- [2] Andrew J Lees. Unresolved issues relating to the shaking palsy on the celebration of james parkinson's 250th birthday. *Movement disorders: official journal of the Movement Disorder Society*, 22(S17):S327–S334, 2007.
- [3] Robert L Nussbaum and Christopher E Ellis. Alzheimer's disease and parkinson's disease. *New england journal of medicine*, 348(14):1356–1364, 2003.
- [4] David T Dexter and Peter Jenner. Parkinson disease: from pathology to molecular disease mechanisms. *Free Radical Biology and Medicine*, 62:132–144, 2013.
- [5] Leslie J Findley. The economic impact of parkinson's disease. *Parkinsonism & related disorders*, 13:S8–S12, 2007.
- [6] Lorraine V Kalia and Anthony E Lang. Parkinson's disease. *The Lancet*, 386(9996):896 – 912, 2015.
- [7] Charles Anthony Davie. A review of parkinson's disease. *British medical bulletin*, 86(1):109–127, 2008.
- [8] Wikipedia contributors. Nigrostriatal pathway. [https://en.wikipedia.org/wiki/File:Nigrostriatal\\_pathway.png](https://en.wikipedia.org/wiki/File:Nigrostriatal_pathway.png), 2015. [Online; accessed -April-2019].
- [9] Werner Poewe, Klaus Seppi, Caroline M Tanner, Glenda M Halliday, Patrik Brundin, Jens Volkmann, Anette-Eleonore Schrag, and Anthony E Lang. Parkinson disease. *Nature reviews Disease primers*, 3:17013, 2017.
- [10] Ricardo Guerrero-Ferreira, Nicholas MI Taylor, Daniel Mona, Philippe Ringler, Matthias E Lauer, Roland Riek, Markus Britschgi, and Henning Stahlberg. Cryo-em structure of alpha-synuclein fibrils. *Elife*, 7:e36402, 2018.
- [11] Anthony HV Schapira, Erwan Bezard, Jonathan Brotchie, Frédéric Calon, Graham L Collingridge, Borris Ferger, Bastian Hengerer, Etienne Hirsch, Peter Jenner, Nicolas Le Novère, et al. Novel pharmacological targets for the treatment of parkinson's disease. *Nature reviews Drug discovery*, 5(10):845, 2006.
- [12] Mojgan Hodaie, Joseph S Neimat, and Andres M Lozano. The dopaminergic nigrostriatal system and parkinson's disease: Molecular events in development, disease, and cell death, and new therapeutic strategies. *Neurosurgery*, 60(1):17–30, 2007.
- [13] Alex Tsui and Ole Isacson. Functions of the nigrostriatal dopaminergic synapse and the use of neurotransplantation in parkinson's disease. *Journal of neurology*, 258(8):1393, 2011.
- [14] Ruwani Wijeyekoon and Roger A Barker. Cell replacement therapy for parkinson's disease. *Biochimica et Biophysica Acta (BBA)-Molecular Basis of Disease*, 1792(7):688–702, 2009.

- [15] Marios Politis, Kit Wu, Clare Loane, Niall P Quinn, David J Brooks, Stig Rehncrona, Anders Bjorklund, Olle Lindvall, and Paola Piccini. Serotonergic neurons mediate dyskinesia side effects in parkinson’s patients with neural transplants. *Science translational medicine*, 2(38):38ra46–38ra46, 2010.
- [16] Ranjita Betarbet, Todd B Sherer, and J Timothy Greenamyre. Animal models of parkinson’s disease. *Bioessays*, 24(4):308–318, 2002.
- [17] Arvid Carlsson, Margit Lindqvist, and TOR Magnusson. 3, 4-dihydroxyphenylalanine and 5-hydroxytryptophan as reserpine antagonists. *Nature*, 180(4596):1200, 1957.
- [18] Kim Tieu. A guide to neurotoxic animal models of parkinson’s disease. *Cold Spring Harbor perspectives in medicine*, 1(1):a009316, 2011.
- [19] Javier Blesa, Sudarshan Phani, Vernice Jackson-Lewis, and Serge Przedborski. Classic and new animal models of parkinson’s disease. *BioMed Research International*, 2012, 2012.
- [20] Fabio Blandini and Marie-Therese Armentero. Animal models of parkinson’s disease. *The FEBS journal*, 279(7):1156–1166, 2012.
- [21] M Flint Beal. Experimental models of parkinson’s disease. *Nature reviews neuroscience*, 2(5):325, 2001.
- [22] Mel B Feany and Welcome W Bender. A drosophila model of parkinson’s disease. *Nature*, 404(6776):394, 2000.
- [23] Michael Galgano, Thomas Russell, Sandra Mc Gillis, Gentian Toshkezi, Lawrence Chin, and Li-Ru Zhao. A review of traumatic brain injury animal models: are we lacking adequate models replicating chronic traumatic encephalopathy. *J Neurol Neurobiol*, 2(1), 2015.
- [24] Sahba Mobini, Young Hye Song, Michaela W. McCrary, and Christine E. Schmidt. Advances in ex vivo models and lab-on-a-chip devices for neural tissue engineering. *Biomaterials*, 198:146 – 166, 2019. Organoids and Ex Vivo Tissue On-Chip Technologies.
- [25] Jared L Sternecker, Peter Reinhardt, and Hans R Schöler. Investigating human disease using stem cell models. *Nature Reviews Genetics*, 15(9):625, 2014.
- [26] Shelley J Allen, Judy J Watson, Deborah K Shoemark, Neil U Barua, and Nikunj K Patel. Gdnf, ngf and bdnf as therapeutic options for neurodegeneration. *Pharmacology & therapeutics*, 138(2):155–175, 2013.
- [27] Sonia Gandhi and Andrey Y Abramov. Mechanism of oxidative stress in neurodegeneration. *Oxidative medicine and cellular longevity*, 2012, 2012.
- [28] Anne M Taylor, Mathew Blurton-Jones, Seog Woo Rhee, David H Cribbs, Carl W Cotman, and Noo Li Jeon. A microfluidic culture platform for cns axonal injury, regeneration and transport. *Nature methods*, 2(8):599, 2005.
- [29] Jeong Won Park, Behrad Vahidi, Anne M Taylor, Seog Woo Rhee, and Noo Li Jeon. Microfluidic culture platform for neuroscience research. *Nature protocols*, 1(4):2128, 2006.

- [30] Sunja Kim, Jaewon Park, Arum Han, and Jianrong Li. Microfluidic systems for axonal growth and regeneration research. *Neural regeneration research*, 9(19):1703, 2014.
- [31] Arseniy Gladkov, Yana Pigareva, Daria Kutyina, Vladimir Kolpakov, Anton Bukatin, Irina Mukhina, Victor Kazantsev, and Alexey Pimashkin. Design of cultured neuron networks in vitro with predefined connectivity using asymmetric microfluidic channels. *Scientific reports*, 7(1):15625, 2017.
- [32] Hyung Joon Kim, Jeong Won Park, Jae Woo Park, Jae Hwan Byun, Behrad Vahidi, Seog Woo Rhee, and Noo Li Jeon. Integrated microfluidics platforms for investigating injury and regeneration of cns axons. *Annals of biomedical engineering*, 40(6):1268–1276, 2012.
- [33] Katherine A Southam, Anna E King, Catherine A Blizzard, Graeme H McCormack, and Tracey C Dickson. Microfluidic primary culture model of the lower motor neuron–neuromuscular junction circuit. *Journal of neuroscience methods*, 218(2):164–169, 2013.
- [34] Eric C Freundt, Nate Maynard, Eileen K Clancy, Shyamali Roy, Luc Bousset, Yannick Sourigues, Markus Covert, Ronald Melki, Karla Kirkegaard, and Michel Brahic. Neuron-to-neuron transmission of  $\alpha$ -synuclein fibrils through axonal transport. *Annals of neurology*, 72(4):517–524, 2012.
- [35] In Hong Yang, Devin Gary, Misti Malone, Stephen Dria, Thierry Houdayer, Visar Belegu, John W Mcdonald, and Nitish Thakor. Axon myelination and electrical stimulation in a microfluidic, compartmentalized cell culture platform. *Neuromolecular medicine*, 14(2):112–118, 2012.
- [36] Ana Villa, Isabel Liste, Elise T Courtois, Emma G Seiz, Milagros Ramos, Morten Meyer, Bengt Juliusson, Philip Kusk, and Alberto Martinez-Serrano. Generation and properties of a new human ventral mesencephalic neural stem cell line. *Experimental cell research*, 315(11):1860–1874, 2009.
- [37] Ana Villa, Beatriz Navarro-Galve, Carlos Bueno, Sonia Franco, Maria A Blasco, and Alberto Martinez-Serrano. Long-term molecular and cellular stability of human neural stem cell lines. *Experimental cell research*, 294(2):559–570, 2004.
- [38] Maria Jose Pino-Barrio, Elisa Garcia-Garcia, Pablo Menendez, and Alberto Martinez-Serrano. V-myc immortalizes human neural stem cells in the absence of pluripotency-associated traits. *PloS one*, 10(3):e0118499, 2015.
- [39] Gina S Fiorini and Daniel T Chiu. Disposable microfluidic devices: fabrication, function, and application. *BioTechniques*, 38(3):429–446, 2005.
- [40] Karina Ziółkowska, Radosław Kwapiszewski, and Zbigniew Brzozka. Microfluidic devices as tools for mimicking the in vivo environment. *New Journal of Chemistry*, 35(5):979–990, 2011.
- [41] Wen-I Wu, Kyla N Sask, John L Brash, and P Ravi Selvaganapathy. Polyurethane-based microfluidic devices for blood contacting applications. *Lab on a Chip*, 12(5):960–970, 2012.
- [42] Pamela N Nge, Chad I Rogers, and Adam T Woolley. Advances in microfluidic materials, functions, integration, and applications. *Chemical reviews*, 113(4):2550–2583, 2013.
- [43] Douglas B Weibel, Willow R DiLuzio, and George M Whitesides. Microfabrication meets microbiology. *Nature Reviews Microbiology*, 5(3):209, 2007.

- [44] Matthias Mehling and Savaş Tay. Microfluidic cell culture. *Current opinion in Biotechnology*, 25:95–102, 2014.
- [45] Michael W Toepke and David J Beebe. Pdm absorption of small molecules and consequences in microfluidic applications. *Lab on a Chip*, 6(12):1484–1486, 2006.
- [46] Keil J Regehr, Maribella Domenech, Justin T Koepsel, Kristopher C Carver, Stephanie J Ellison-Zelski, William L Murphy, Linda A Schuler, Elaine T Alarid, and David J Beebe. Biological implications of polydimethylsiloxane-based microfluidic cell culture. *Lab on a Chip*, 9(15):2132–2139, 2009.
- [47] Jessamine Ng Lee, Cheolmin Park, and George M Whitesides. Solvent compatibility of poly (dimethylsiloxane)-based microfluidic devices. *Analytical chemistry*, 75(23):6544–6554, 2003.
- [48] Larry J Millet, Matthew E Stewart, Jonathan V Sweedler, Ralph G Nuzzo, and Martha U Gillette. Microfluidic devices for culturing primary mammalian neurons at low densities. *Lab on a Chip*, 7(8):987–994, 2007.
- [49] Tharkika Nagendran, Valerie Poole, Joseph Harris, and Anne Marion Taylor. Use of pre-assembled plastic microfluidic chips for compartmentalizing primary murine neurons. *JoVE (Journal of Visualized Experiments)*, (141):e58421, 2018.
- [50] Kangning Ren, Jianhua Zhou, and Hongkai Wu. Materials for microfluidic chip fabrication. *Accounts of chemical research*, 46(11):2396–2406, 2013.
- [51] Holger Becker. It’s the economy. . . . *Lab on a Chip*, 9(19):2759–2762, 2009.
- [52] David J Guckenberger, Theodorus E de Groot, Alwin MD Wan, David J Beebe, and Edmond WK Young. Micromilling: a method for ultra-rapid prototyping of plastic microfluidic devices. *Lab on a Chip*, 15(11):2364–2378, 2015.
- [53] Arshya Bamshad, Alireza Nikfarjam, and Hossein Khaleghi. A new simple and fast thermally-solvent assisted method to bond pmma–pmma in micro-fluidics devices. *Journal of Micromechanics and Microengineering*, 26(6):065017, 2016.
- [54] Ansgar Waldbaur, Holger Rapp, Kerstin Länge, and Bastian E Rapp. Let there be chip—towards rapid prototyping of microfluidic devices: one-step manufacturing processes. *Analytical Methods*, 3(12):2681–2716, 2011.
- [55] Anthony K Au, Wonjae Lee, and Albert Folch. Mail-order microfluidics: evaluation of stereolithography for the production of microfluidic devices. *Lab on a Chip*, 14(7):1294–1301, 2014.
- [56] Johan U Lind, Travis A Busbee, Alexander D Valentine, Francesco S Pasqualini, Hongyan Yuan, Moran Yadid, Sung-Jin Park, Arda Kotikian, Alexander P Nesmith, Patrick H Campbell, et al. Instrumented cardiac microphysiological devices via multimaterial three-dimensional printing. *Nature materials*, 16(3):303, 2017.
- [57] Mutsuyuki Sugimori and Rodolfo R Llinas. Real-time imaging of calcium influx in mammalian cerebellar purkinje cells in vitro. *Proceedings of the National Academy of Sciences*, 87(13):5084–5088, 1990.

- [58] Yehezkel Ben-Ari, Jean-Luc Gaiarsa, Roman Tyzio, and Rustem Khazipov. Gaba: a pioneer transmitter that excites immature neurons and generates primitive oscillations. *Physiological reviews*, 87(4):1215–1284, 2007.
- [59] Ana Villa, Evan Y Snyder, Angelo Vescovi, and Alberto Martainez-Serrano. Establishment and properties of a growth factor-dependent, perpetual neural stem cell line from the human cns. *Experimental neurology*, 161(1):67–84, 2000.
- [60] Takuma Kumamoto and Carina Hanashima. Evolutionary conservation and conversion of foxg1 function in brain development. *Development, growth & differentiation*, 59(4):258–269, 2017.
- [61] KC Langley, C Bergson, P Greengard, and CC Ouimet. Co-localization of the d1 dopamine receptor in a subset of darpp-32-containing neurons in rat caudate–putamen. *Neuroscience*, 78(4):977–983, 1997.
- [62] P Svenningsson, M Lindskog, F Rognoni, BB Fredholm, P Greengard, and G Fisone. Activation of adenosine a2a and dopamine d1 receptors stimulates cyclic amp-dependent phosphorylation of darpp-32 in distinct populations of striatal projection neurons. *Neuroscience*, 84(1):223–228, 1998.
- [63] Eun-Hye Joe, Dong-Joo Choi, Jiawei An, Jin-Hwa Eun, Ilo Jou, and Sangmyun Park. Astrocytes, microglia, and parkinson’s disease. *Experimental neurobiology*, 27(2):77–87, 2018.
- [64] Heather DE Booth, Warren D Hirst, and Richard Wade-Martins. The role of astrocyte dysfunction in parkinson’s disease pathogenesis. *Trends in Neurosciences*, 40(6):358–370, 2017.
- [65] Beatriz de Lucas, Laura M Pérez, and Beatriz G Gálvez. Importance and regulation of adult stem cell migration. *Journal of cellular and molecular medicine*, 22(2):746–754, 2018.
- [66] Eric Wildon Kostuk, Jingli Cai, and Lorraine Iacovitti. Regional microglia are transcriptionally distinct but similarly exacerbate neurodegeneration in a culture model of parkinson’s disease. *Journal of neuroinflammation*, 15(1):139, 2018.
- [67] Elise T Courtois, Claudia G Castillo, Emma G Seiz, Milagros Ramos, Carlos Bueno, Isabel Liste, and Alberto Martinez-Serrano. In vitro and in vivo enhanced generation of human a9 dopamine neurons from neural stem cells by bcl-xl. *Journal of Biological Chemistry*, 285(13):9881–9897, 2010.



**Erklärung zur wissenschaftlichen Redlichkeit**  
(beinhaltet Erklärung zu Plagiat und Betrug)

~~Bachelorarbeit / Masterarbeit~~ (nicht Zutreffendes bitte streichen)

Titel der Arbeit (Druckschrift):

Two Dimensional Brain-on-chip Model  
Towards Remodelling of the nigrostriatal Pathway  
to Study Parkinson's Disease

Name, Vorname (Druckschrift): Sebastian Buchmann

Matrikelnummer: 19-053-474

Hiermit erkläre ich, dass mir bei der Abfassung dieser Arbeit nur die darin angegebene Hilfe zuteil wurde und dass ich sie nur mit den in der Arbeit angegebenen Hilfsmitteln verfasst habe.

Ich habe sämtliche verwendeten Quellen erwähnt und gemäss anerkannten wissenschaftlichen Regeln zitiert.

Diese Erklärung wird ergänzt durch eine separat abgeschlossene Vereinbarung bezüglich der Veröffentlichung oder öffentlichen Zugänglichkeit dieser Arbeit.

ja  nein

Ort, Datum: Kopenhagen 3.5.19

Unterschrift: T. Buhl

Dieses Blatt ist in die Bachelor-, resp. Masterarbeit einzufügen.